

**Sea ice break-up and freeze-up indicators for users
of the Arctic coastal environment**

John E. Walsh¹, Hajo Eicken¹, Kyle Redilla¹, Mark Johnson²

¹International Arctic Research Center, University of Alaska Fairbanks, Fairbanks AK 99775
USA

²College of Fisheries and Ocean Sciences, University of Alaska Fairbanks, Fairbanks AK
99775 USA

Correspondence to: John E. Walsh (jewalsh@alaska.edu)

Formatted

Deleted: ¶

Formatted: Left

Deleted: ¶

Deleted: January 2022¶
Submitted

Deleted: to

July 2022
Revision for *The Cryosphere*

Abstract

The timing of sea ice retreat and advance in Arctic coastal waters varies substantially from year to year. Various activities, ranging from marine transport to the use of sea ice as a platform for industrial activity or winter travel, are affected by variations in the timing of break-up and freeze-up, resulting in a need for indicators to document the regional and temporal variations in coastal areas. The primary objective of this study is to use locally-based metrics to construct indicators of break-up and freeze-up in the Arctic/Subarctic coastal environment. The indicators developed here are based on daily sea ice concentrations derived from satellite passive microwave measurements. The “day of year” indicators are designed to optimize value for users while building on past studies characterizing break-up and freeze-up dates in the open pack ice. Relative to indicators for broader adjacent seas, the coastal indicators show later break-up at sites known to have extensive landfast ice. The coastal indicators also show earlier freeze-up at some sites in comparison with freeze-up for broader offshore regions, likely tied to earlier freezing of shallow water regions and areas affected by freshwater input from nearby streams and rivers. A factor analysis performed to synthesize the local indicator variations shows that the local break-up and freeze-up indicators have greater spatial variability than corresponding metrics based on regional ice coverage. However, the trends towards earlier break-up and later freeze-up are unmistakable over the post-1979 period in the synthesized metrics of the coastal break-up/freeze-up and the corresponding regional ice coverage. The findings imply that locally defined indicators can serve as key links between pan-Arctic or global indicators such as sea-ice extent or volume and local uses of sea ice, with the potential to inform community-scale adaptation and response.

Key words: sea ice, Arctic, break-up, freeze-up, ice concentration

Deleted: ¶
¶

Deleted: Arctic coastal waters are characterized by seasonal retreat and advance of sea ice.

Deleted: advance and retreat

Deleted:

Deleted: u

Deleted: Here we develop indicators

Deleted:

Deleted: , for which break-up typically lags retreat of the adjacent, thinner drifting ice

Deleted: an

Deleted: ir

1. Introduction

Coastal sea ice impacts residents and other users of the [nearshore marine](#) environment in various ways. Perhaps most obvious is the fact that non-ice strengthened vessels require ice-free waters for marine transport, which can serve purposes such as resupply of coastal communities, the transport of extracted resources (oil, liquefied natural gas, mined metals), migration of marine mammals (e.g., bowhead whales) and wintertime travel over the ice by coastal residents. Key metrics for [such uses of the nearshore marine environment](#) are the timing of break-up (or ice retreat) in the spring and the timing of freeze-up (or ice advance) in the autumn or early winter.

Sea ice concentration [thresholds have been used in various studies to determine the dates of sea ice opening, retreat, advance and closing](#) (Markus et al., 2009; Johnson and Eicken, 2016; Bliss and Anderson, 2018; Peng et al., 2018; [Bliss et al., 2019](#); Smith and Jahn, 2019). For example, [Bliss et al. \(2019\) define dates of opening and retreat as, respectively, the last days on which the sea ice concentration drops below 80% and 15% before the summer minimum. Corresponding metrics are used by Bliss et al. for the dates of advance and closing.](#) An emerging tendency in these [and similar](#) studies is the definition of break-up date as the date on which ice concentration drops below a prescribed threshold and remains below that threshold for a prescribed minimum duration (chosen to eliminate repeated crossings of the concentration threshold as a result of temperature- or wind-driven changes in ice coverage associated with transient weather events). A corresponding criterion is used for the freeze-up date.

Coastal regions present special challenges in the application of such criteria. First, shorefast or landfast ice (stationary sea ice held in place along the shoreline [as a result of grounding](#)

Deleted: offshore

Deleted: offshore uses

Deleted: such as these

Deleted: is the basis of most metrics of the timing (dates) of sea ice break-up and freeze-up

Deleted: Bliss et al., 2019;

Deleted: through

and/or confinement by the coast) is common in waters immediately offshore of the coast, particularly in areas with shallow water. Landfast ice provides especially important sea ice services because it offers a stable platform for nearshore travel, serves as a critical habitat for marine mammals such as seals and polar bears (Dammann et al., 2018), and provides a buffer against coastal storms (Hosekova et al., 2021). Second, sea ice concentrations derived from passive microwave measurements are prone to contamination by microwave emissions from land in coastal grid cells. Finally, many parts of the Arctic coastline have inlets, river deltas and barrier islands that are not captured by the 25 km resolution of the passive microwave product. While higher-resolution datasets permitting finer resolution of coastal sea ice are available from sensors such as AMSR (Advanced Microwave Scanning Radiometer), the record lengths are sufficiently shorter (about 20 years for AMSR) that trend analyses are limited by a reliance on such products. Trend analysis is one of the main components of the present study.

The primary objective of this study was to use the locally-based metrics to construct indicators of break-up and freeze-up on Arctic/Subarctic coastal environments. A subcomponent of this overall objective is to contribute to efforts at the national and global scale to establish key sets of indicators that support sustained assessment of climate change and inform planning and decision-making for adaptation action (AMAP, 2018; IPCC, 2022). At the global, pan-Arctic, and U.S. national levels, indicators associated with the state of the sea ice cover so far have focused on the summer minimum and winter maximum extent and ice thickness (IPCC, 2022; AMAP, 2017; Box et al., 2019; USGCRP, 2017). As outlined by Box et al. (2019), this approach has been motivated by the objective of describing and tracking the state of key components of the global climate system. However, large-scale (pan-

Commented [MAJ1]: Just because you use especially in the next sentence....

Deleted: especially

Deleted: Shorefast

Deleted: offshore

Commented [MAJ2]: This may be where you can add language on the landfast ice mask issues that Kyle has mentioned in our recent emails....

Deleted: A key aim of the current study is

Deleted: Kenney et al., 2016;

Deleted: Both at

Deleted: and

Deleted: global, as well as the

Deleted: Box et al., 2019; IPCC, 2022

Arctic) measures of e.g., sea-ice extent or volume are of little value and relevance to those needing to adapt or respond to such change at the community or regional scale. Here, we examine the timing of sea-ice freeze-up and break-up as key constraints for a range of human activities and ecosystem functions in Arctic settings.

2. Data and methods

The primary data source is the archive of gridded daily sea ice concentrations derived from the SMMR, SSM/I and SSMIS sensors onboard the Nimbus-7 and various DMSP satellites dating back to November, 1978. The dataset is NSIDC-0051 of the National Snow and Ice Data Center (NSIDC), and is accessible at <https://nsidc.org/data/nsidc-0051>. In the construction of this dataset, the NASA Team algorithm (Cavalieri et al., 1984) and the NASA Bootstrap algorithm (Comiso et al., 1986) were used to process the microwave brightness temperatures into a consistent time series of daily sea ice concentrations. The data are on a polar stereographic grid projection with a grid cell size of 25 km x 25 km. Prior to applying these definitions, the data were processed with a linear interpolation to fill in missing daily values, followed by a spatial and then temporal smoothing to filter out short (< 3 days) events. Specifically, the daily sea ice concentration values were spatially smoothed using a generic mean filter with a square footprint of 3 x 3 grid cells. The data were then temporally smoothed three times using a Hann window.

The daily sea ice concentrations are used to define the metrics of the start and end of break-up and freeze-up in each year of a 40-year period, 1979-2018. The definitions build on those used by Johnson and Eicken (2016; hereafter denoted as J&E), which were informed by Indigenous experts' observations of ice use and ice hazards in coastal Alaska, and relate to planning and decision-making at the community-scale (Eicken et al., 2014). Here, we expand

Deleted: used here

Deleted: ,

Deleted: , is the NOAA/NSIDC Climate Data Record of Passive Microwave Sea Ice Concentration Version 3.

Field Code Changed

the satellite data analysis with minor modifications of the break-up and freeze-up criteria to broaden the applicability to coastal areas. Examples include imposing maximum and minimum values for the thresholds computed from summary statistics of the daily sea ice concentration values of relevant periods. The revised definitions are presented in Table 1 and the differences relative to those of J&E are listed in Table 2.

Deleted: non-

While the various thresholds in Table 1 may seem somewhat arbitrary at first glance, they are based on past studies and subsequent sensitivity tests. In particular, the 10% threshold is based on prior work (J&E) in which sensitivities were explored. The 25%, 40% and 50% thresholds in Table 1 were arrived at by testing various values and selecting values that maximized the number of years with break-up and defined freeze-up dates and had the best agreement with years of indigenous observations. The selected values were those that generally maximized the number of such years across the various coastal locations and MASIE regions.

Formatted: Space Before: Auto, After: Auto

Table 1. Definition of the start and end of break-up and freeze-up.

Break-up start	The date of the last day for which the previous two weeks' ice concentration always exceeds a threshold computed as the maximum of (a) the winter (January-February) average minus two standard deviations and (b) 15%. Undefined if the average summer sea ice concentration (SIC) is greater than 40% or if the subsequent break-up end is not defined.
Break-up end	The first date after the break-up start date for which the ice concentration during the following two weeks is less than a threshold computed as the maximum of (a) the summer (August-September) average plus one standard deviation and (b) 50%. Undefined if the daily SIC is less than the threshold for the entire summer or if break-up start is not defined.
Freeze-up start:	The date on which the ice concentration exceeds for the first time a threshold computed as the maximum of (a) the summer (August-September) average plus one standard deviation and (b) 15%. Undefined if the daily SIC never exceeds this threshold, if the mean summer SIC is greater than 25%, or if subsequent freeze-up end is not defined.
Freeze-up end:	The first date after the freeze-up start date for which the following two weeks' ice concentration exceeds a threshold computed as the maximum of (a) the average winter (January-February) ice concentration minus 10% and (b) 15%, and the minimum of this result and (c) 50%. Undefined if daily SIC exceeds this threshold for every day of the search period or if freeze-up start is not defined.

Table 2. Changes in the indicator definitions relative to Johnson and Eicken (2016), denoted as “J&E”. The symbol “ σ ” denotes standard deviation; “sic” denotes sea ice concentration.

Formatted: Left

Break-up start:

Formatted: Line spacing: Double

- minimum sic threshold created at 15% (J&E: last day exceeding Jan-Feb mean minus 2σ)
- undefined if average summer sic > 40% (J&E: no such criterion)
- undefined if subsequent breakup end date not defined (J&E: no such criterion)

Break-up end:

- first time sic below threshold for 2 weeks instead of last day below threshold

(J&E: last exceeding larger of Aug-Sep mean or 15%)

Deleted: .

- minimum threshold 50% (J&E: minimum threshold of 15%)
- undefined if break-up start not defined (J&E: no such criterion)

Freeze-up start:

- first day on which sic exceeds Aug-Sep average by 1σ (J&E: same)
- undefined if mean summer sic > 25% (J&E: no such criterion)
- undefined if subsequent freeze-up end not defined (J&E: same)

Freeze-up end:

- first time sic above threshold for following 2 weeks instead of first day above threshold
(threshold is Jan-Feb average minus 10%, as in J&E)
- thresholds imposed: Minimum (15%) and maximum (50%) (J&E: no such thresholds)
- undefined if sic always exceeds threshold (J&E: same)

Our evaluation of the coastal indicators includes comparisons of the various dates (break-up/freeze-up start/end) at nearshore locations with the corresponding metrics for broader areas of the Arctic Ocean and the subarctic seas. A set of ten locations was selected on the basis of their geographical distribution and the relevance of local sea ice to uses by communities, industry, military or other stakeholders. These locations are listed in Table 3, together with their geographic coordinates. While there is admittedly some subjectivity in the selection of these sites, our priorities were (1) a pan-Arctic geographical distribution, thereby expanding the emphasis on North American locations in past studies (see Discussion in Section 4) and (2) inclusion of locations with a mix of users affected by sea ice: Indigenous communities, industry, military and other stakeholders. For each of these locations, several passive microwave grid cells close to (but not adjacent to) the coastline were selected for calculation of the break-up and freeze-up metrics. More specifically, the contamination of the passive microwave-derived ice concentrations by the presence of land in a grid cell required the exclusion of grid cells containing land. Therefore, the selected grid cells satisfied the criterion that they were the cells closest to the coast but centered at least 25 km from the coast. Figure 1 shows geographical insets illustrating the proximity of the selected grid cells to the coastline.

With regard to the grid cell selection, we experimented with the grid cell selections at Sabetta and Utqiagvik. When the grid cell locations were one shifted offshore by one pixel at Sabetta, the mean break-up start and end dates changed by only -0.1 and -1.1 days, respectively; the corresponding changes in the freeze-up start and end dates were 0.2 and -0.7 days, respectively. At Utqiagvik, the offshore shift resulted in an earlier mean break-up start by 3.3 days and a later mean break-up end by 2.9 days. The earlier break-up start is consistent with

Deleted: Prior to applying these definitions, the data were processed with a linear interpolation to fill in missing daily values, followed by a spatial and then temporal smoothing to smooth out short (< 3 days) events.¶
A key objective of this work is to

Formatted: Space Before: Auto, After: Auto

Deleted: compare

Deleted: 2

Commented [MAJ4]: In the Review Response you write “we actually experimented with the grid cell selections at Utqiagvik and Sabetta. The trends and interannual variations of the break-up start and freeze-up end showed no notable changes (i.e., no change exceeded 2 days) when the three selected grid cells were displaced offshore or alongshore by one grid cell.” Is it worthwhile adding some version of this statement here to clarify the sensitivity of our results to grid-cell location choices?

Formatted: Font: (Default) Times New Roman

Formatted: Font: (Default) Times New Roman

the presence of fast ice at the coast, as discussed in Section 4. The changes in Utqiagvik’s freeze-up dates were small when the pixels were shifted offshore, where the start of freeze-up occurred 1.1 days later and the end of freeze-up 1.1 days earlier than closer to the coast.

Table 3. Near-coastal locations selected for calculation of break-up and freeze-up metrics

<u>Sea</u>	<u>Location</u>	<u>Latitude, Longitude</u>	<u>Significance of location</u>
Beaufort Sea	Prudhoe Bay	70.2N, 148.2W	oil facilities
Chukchi/Beaufort Seas	Utqiagvik	71.3N, 156.8W	Indigenous community
Chukchi Sea	Chukchi Sea	69.6N, 170W	shipping route
Bering Sea	St. Lawrence Island	65.7N, 168.4W	Indigenous community
East Siberian Sea	Pevek	69.8N, 170.6E	port, mining facility
Laptev Sea	Tiksi	71.7N, 72.1E	research site, port
Kara Sea	Sabetta	71.3N, 72.1E	port, LNG facility
Greenland Sea	Mestersvig	72.2N, 23.9W	military base
Baffin Bay	Clyde River	70.3N, 68.3W	Indigenous community
Hudson Bay	Churchill	58.8N, 94.2W	port, tourism

Deleted: ¶

Table 1. Definition of the start and end of break-up and freeze-up.¶

Break-up start The date of the last day for which the previous two weeks’ ice concentration always exceeds a threshold computed as the maximum of (a) the winter (January-February) average minus two standard deviations and (b) 15%. Undefined if the average summer sea ice concentration (SIC) is greater than 40% or if the subsequent break-up end is not defined.¶

Break-up end The first date after the break-up start date for which the following two weeks’ ice concentration is less than a threshold computed as the maximum of (a) the summer (August-September) average plus one standard deviation and (b) 50%. Undefined if the daily SIC is less than the threshold for the entire summer or if break-up start is not defined.¶

Freeze-up start: The date on which the ice concentration exceeds for the first time a threshold computed as the maximum of (a) the summer (August-September) average plus one standard deviation and (b) 15%. Undefined if the daily SIC never exceeds this threshold, if the mean summer SIC is greater than 25%, or if subsequent freeze-up end is not defined.¶

Freeze-up end: The first date after the freeze-up start date for which the following two weeks’ ice concentration exceeds a threshold computed as the maximum of (a) the average winter (January-February) ice concentration minus 10% and (b) 15%, and the minimum of this result and (c) 50%. Undefined if daily SIC exceeds this threshold for every day of the search period or if freeze-up start is not defined.¶

Formatted: Indent: Left: 0", First line: 0"

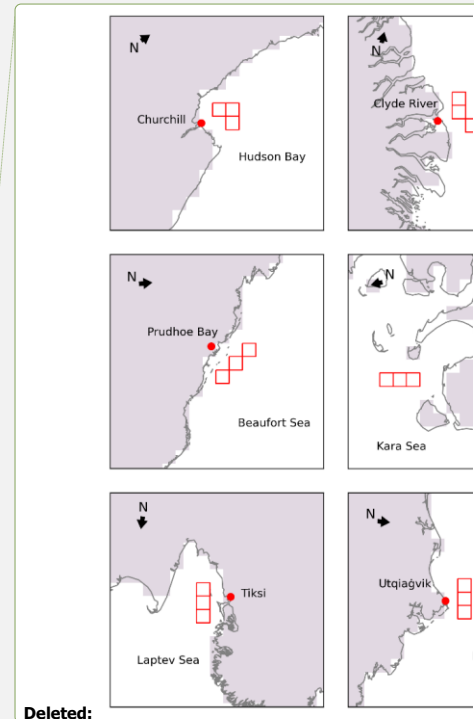
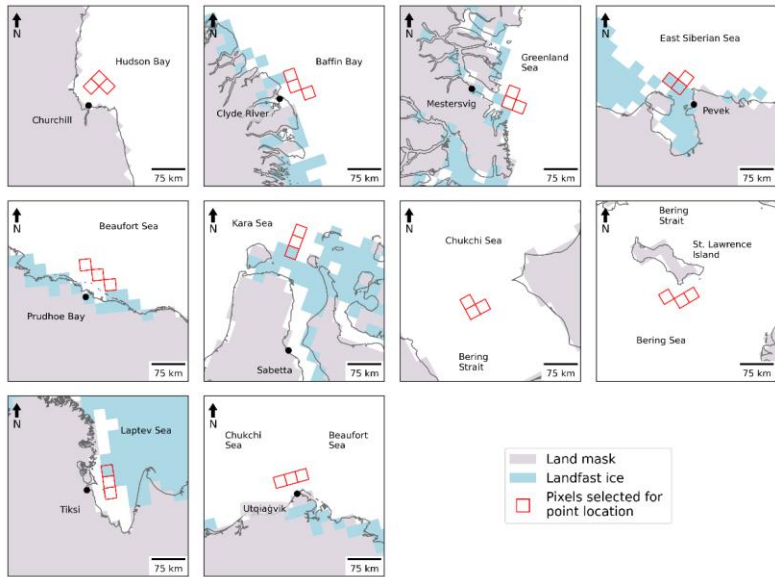
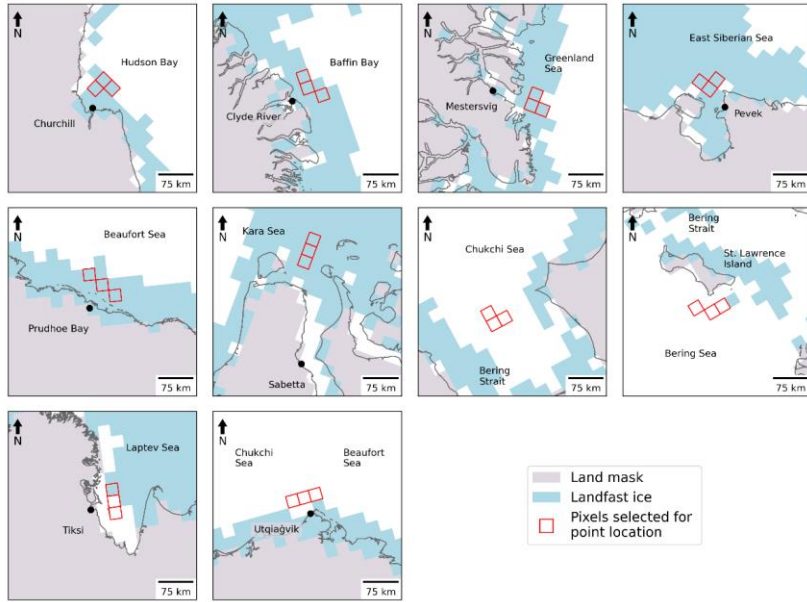
Deleted: 2

Formatted: Space After: 12 pt

Deleted:

Deleted: Bering Strait coast

Deleted:



Deleted:

Figure 1. Grid cells (red squares) for which passive-microwave-derived ice concentrations were used in computing the break-up and freeze-up metrics for the coastal locations. Black dots represent the actual locations of the coastal communities. Blue shading denotes maximum (upper panels) and median (lower panels) coverage of landfast ice in June over the 1972-2007 period based on charts of the U.S. National Ice Center -- <https://nsidc.org/data/G02172> (accessed 28 June 2022).

It is apparent from Figure 1 that the innermost extent of the landfast ice does not always coincide with the coastline. The northern Siberian coast (Sabetta and Tiksi) provides examples. In pursuing an explanation for the discrepancies, we found that the land mask in the fast ice dataset (digitized charts of the National Ice Center) differs from the land mask of the NSIDC's passive microwave dataset. The resulting offset does not change the area covered by sea ice in each regional plot, but it does result in the mis-location of the nearshore edge. The discrepancy does not alter the reasoning about the geographically varying roles of landfast ice, as discussed in Section 4.

The grid cell selections for St. Lawrence Island and the Chukchi Sea deserve special comment. The grid cells off St. Lawrence Island were chosen to reflect timing and location of subsistence harvests by the communities of Gambell and Savoonga. Because of extensive ice coverage, including landfast ice, north and northwest of the island, both communities traditionally conduct bowhead whale harvests at hunting camps on the south side of the island once spring ice break-up is underway (Noongwook et al., 2007). These sites also reflect the seasonal migration of whales in waters south of the island with the seasonal retreat of the ice cover (Noongwook et al., 2007), modulated somewhat by the presence of a polynya south and

Formatted: Space After: 24 pt

Deleted: used for sea ice indicator metrics corresponding to coastal locations (red dots).

Commented [JWJ5]: Kyle: Is that correct?

Formatted: Font:

Deleted: Previous studies cited earlier have evaluated break-up and freeze-up metrics for subregions of the Arctic Ocean and the surrounding seas. For comparisons with similar regions, we utilize the MASIE (Multisensor Analyzed Sea Ice Extent) regionalization (https://nsidc.org/data/masie/browse_regions). Of the MASIE regions shown in Figure 1, we choose the following for computation of regionally averaged metrics of break-up and freeze-up: (1) Beaufort Sea, (2) Chukchi Sea, (3) East Siberian Sea, (4) Laptev Sea, (5) Kara Sea, (6) Barents Sea, (7) Greenland Sea, (8) Baffin Bay, (9) Canadian Archipelago, (10) Hudson Bay, (11) Central Arctic and (12) Bering Sea.¶

southwest of the island (Krupnik et al., 2010; Noongwook et al., 2007). Traditional walrus harvest practices on St. Lawrence Island await the very end of the bowhead whale hunt (Kapsch et al., 2010), with timing of spring ice break-up south of the island as the driving factor. These practices motivated our selection of grid cells southeast of the island. As shown later (Section 4), landfast ice is confined to the northern coastal region of St. Lawrence Island – consistent with the frequent presence of the polynya south of the island. In the case of the Chukchi Sea, the grid cells are indeed farther from the coast than for the other sites; the locations were intentionally selected to be farther offshore in order to provide a non-coastal counter-example to the other sites, all of which are adjacent to a coast.

Commented [MAJ7]: This section above is really nice and addresses well the comments of the reviewer.

Previous studies cited earlier have evaluated break-up and freeze-up metrics for subregions of the Arctic Ocean and the surrounding seas (Markus et al., 2006; Johnson and Eicken, 2016; Bliss and Anderson, 2018; Peng et al., 2018; Bliss et al., 2019; Smith and Jahn, 2019). For comparisons with broader regions offshore of our selected sites, we utilize the MASIE (Multisensor Analyzed Sea Ice Extent) regionalization (https://nsidc.org/data/masie/browse_regions). Of the MASIE regions shown in Figure 2, we choose the following for computation of regionally averaged metrics of break-up and freeze-up: Beaufort Sea, Chukchi Sea, East Siberian Sea, Laptev Sea, Kara Sea, Greenland Sea, (8) Baffin Bay, Hudson Bay, and Bering Sea.

Formatted: Indent: First line: 0"

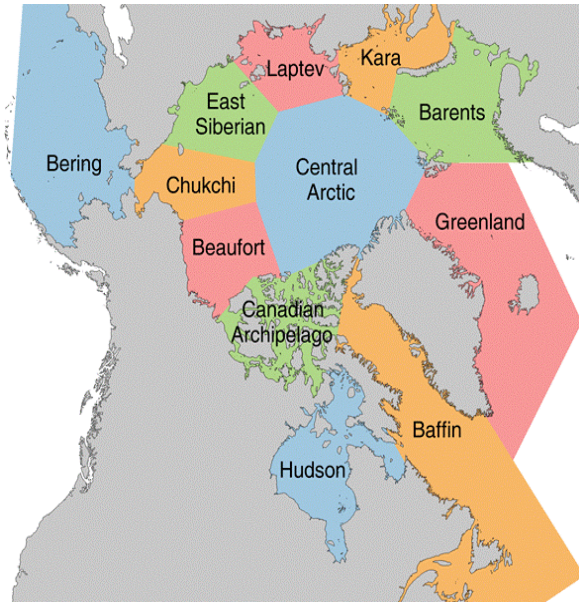
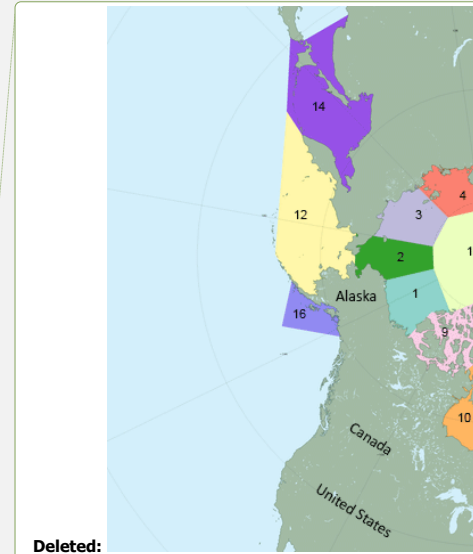


Figure 2. The MASIE subregions of the Arctic. Regions utilized in this study include Beaufort Sea, Chukchi Sea, East Siberian Sea, Laptev Sea, Kara Sea, Baffin Bay, Hudson Bay, and Bering Sea.

The following section includes time series of the local indicators and, for comparison, time series of the corresponding MASIE regional indicators. In order to address the spatial coherence of the indicators, we performed a factor analysis on the different sets (break-up/freeze-up, start/end dates). The computation of the indicators was done for the ten local sites and for the MASIE regions in which they fall. Factor analysis is a statistical method for quantifying relationships among a set of variables. The variability in the overall dataset is depicted by a set of factors. Each factor explains a percentage of the total variance in space and time. Each variable in each factor is given a loading (or weight) based on its contribution to the variance explained by that factor. The first factor can be viewed as the linear



Deleted:

Deleted: (see Table 2)

Deleted: #s 1

Deleted: (

Deleted:)

Deleted: 2 (

Deleted:), 3 (

Deleted:), 4 (

Deleted:), 5 (

Deleted:), 7 (

Deleted: Greenland Sea), 8 (

Commented [MAJ8]: This list is different from page 12, bottom. This one is missing Barents Sea, Canadian Archipelago, a ...

Commented [JWJ9R8]: List in text above figure has been corrected.

Deleted: Baffin Bay), 10 (Hudson

Deleted:) and 12 (

Deleted:).

Deleted: ¶

Deleted:

Commented [MAJ11]: Does this help clarify the shift from 16 to the 12 regions in Fig 4? I had to re-read this a couple times...ls ...

Commented [JWJ12R11]: Changed the figure and the text for consistency, as suggested by Mark

Commented [JWJ13R11]:

Deleted: of ten regional indicators. (MASIE regions 13, 14, 15, and 16 are not relevant to this study.)

combination of the variables that maximizes the explained variance in the overall dataset. The second and each successive factor maximize the variance unexplained by the preceding factors. Successive factors explain successively smaller fractions of the overall variance. Multiple variables can have strong loadings in the same factor, indicating they follow a similar pattern and are likely highly related. Factor analysis has a long history of applications to Arctic sea ice variability (Walsh and Johnson, 1982; Fang and Wallace, 1994; Deser et al., 2000; Fu et al., 2021). The factor analysis calculations used here were performed using the XLSAT software package run in Excel (<https://www.xlstat.com/en/>)

3. Results

With coastal ice retreat and onset of ice advance as this study's primary focus, we first demonstrate the applicability of the indicators evaluated here. The various metrics of sea ice break-up and freeze-up in Table 1 are not defined for all locations in the Arctic. For example, locations that remain ice-covered throughout a particular year will not be assigned dates for any of the indicators in that year, and the same is true of locations at which sea ice does not form during a particular year. Figure 3 shows the number of years in the 1979-2018 study period during which the break-up and freeze-up indicators are actually defined. It is apparent that the indicators are consistently defined in the seasonal sea ice zone spanning the subarctic seas. In particular, all ten coastal locations in Table 2 are in the yellow areas (>35 years out of 40 years defined) of Figure 3. Of note in Figure 3 is that the number of years with defined break-up indicators slightly exceeds (by one) the number of years with freeze-up indicators at some locations at the outer periphery of the seasonal sea ice zone. These are locations in which sea ice was present for some portion of the early years but not at the end of the study period, so in one of the years there was a break-up but no freeze-up.

Deleted: s

Deleted: us

Deleted: 2

Deleted:

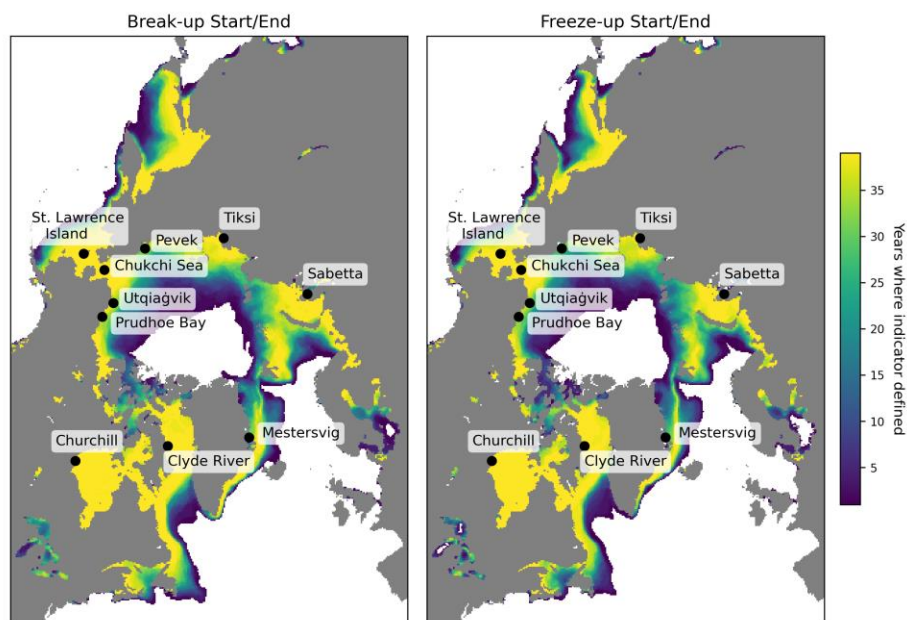


Figure 3. Number of years in the 1979-2018 study period in which the break-up and freeze-up indicators were defined. Note that end dates for break-up and freeze-up exist only for years in which there are start dates for break-up and freeze-up. The start and end dates of the overall data record (1 Jan 1979 – 31 Dec 2018) can result in differences of 1 year in the counts when freeze-up occurs around January 1.

A key issue to be addressed is the degree to which the indicators utilized here differ from those of previous studies. The metrics of Bliss et al. (2019) or similar variants have been used in recent publications and provide natural points of comparison. While there are various differences between our metrics and those of Bliss et al., the most consequential for the computed dates is the use of departures from winter/summer averages concentrations in our criteria vs. Bliss et al.'s use of 15% and 80% concentrations as key thresholds. This

Deleted: ¶

Break-up Start/End

Formatted: Space After: 18 pt

Deleted: ¶

distinction is analogous to the difference between the NASA Team algorithm's use of fixed tie points and the NASA Bootstrap algorithm's use of "dynamic (time/space-varying) tie points".

Commented [MAJ14]: Excellent addition.

The four indicators in this study are the dates of the start and end of break-up and freeze-up. The corresponding indicators used by Bliss et al. (2019) are the date of opening (defined as the last day on which the ice concentration drops below 80% before the summer minimum), the date of retreat (defined as the last day the ice concentration drops below 15% before the summer minimum), the date of advance (defined as the first day the ice concentration increases above 15% following the final summer minimum) and the date of closing (defined as the first day the ice concentration increases above 80% following the final summer minimum). Figure 4 and Table S1 show that there are systematic differences between our metrics (based on J&E) and those of Bliss et al. when the two sets of metrics are evaluated for the MASIE regions. In particular, J&E's start and end of breakup generally occur earlier by up to several weeks than the corresponding dates of opening and retreat defined by Bliss et al. On the other hand, J&E's freeze-up dates are more closely aligned with those of Bliss et al., although J&E's end-of-freeze-up occurs later (by 1 to 3 weeks) than Bliss et al.'s closing date in most of the MASIE regions, especially the North Atlantic and Canadian regions.

Deleted: s

Deleted: Johnson and Eicken, 2016; hereafter denoted as

The violin plots in Figure 4 show distributions but not the temporal variations that have been indicated by results of previous studies (Peng et al., 2018; Bliss et al., 2019). Figures 5 and 6 provide the temporal perspective on the end dates of break-up (Day of retreat) and freeze-up (Day of closing), respectively. In each of the MASIE regions, the J&E criterion gives an earlier break-up date. The difference is typically two to three weeks, although it exceeds a month in the Greenland Sea and Baffin Bay. Despite the offsets, the trends are nearly the

same in nearly all the regions. Exceptions are the Canadian Archipelago, where the J&E trend is weaker than the Bliss trend, and the Bering Sea, where the trends are opposite in sign. However, the trend in the Bering region is not statistically significant at the 99% level by either metric, in contrast to all other regions in which the trends are significant at this level (Table S2). The main conclusion from Figure 5 is that, except for the Bering Sea, sea ice break-up is occurring earlier throughout the Arctic than several decades ago, no matter which metric is used.

In contrast to the trends towards earlier breakup, the J&E and Bliss metrics for the end of freeze-up both show significant trends towards later dates in most of the MASIE regions (Figure 6 and Table S3). In this case, even the Bering Sea shows a trend towards later freeze-up. Again, there is an offset towards a later date with the J&E metric, although the offset has a range among the regions, from essentially zero in Hudson Bay to more than six weeks in the Greenland Sea. The trends, however, show less agreement in some regions than do the trends for break-up dates in Figure 5. The J&E trends are more strongly positive in the seas of the eastern Russian sector: the Chukchi, East Siberian and Laptev Seas. The same is true, although to a lesser degree, in the Barents Sea and the Canadian Archipelago. The main message from Figure 6 is that the freeze-up is ending later throughout the Arctic, although the magnitude of the trend is more sensitive to the criteria used for end-of-freeze-up than for end-of-break-up.

Deleted: .

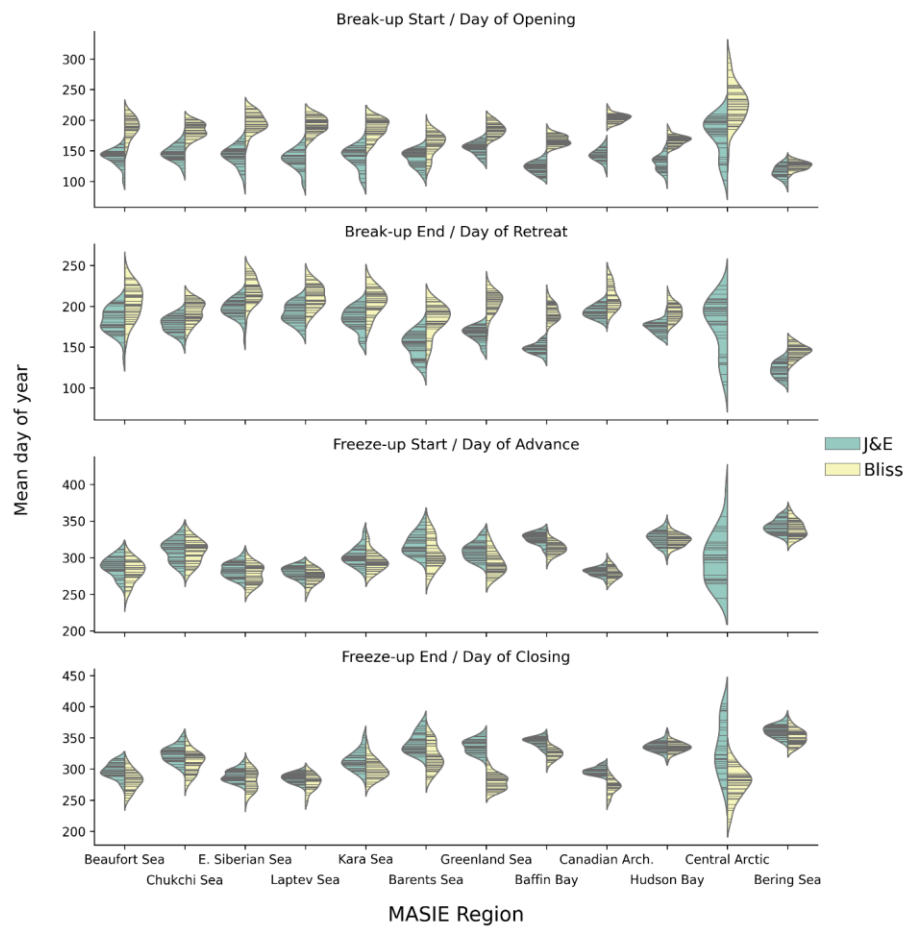


Figure 4. “Violin” plots of the Julian dates of the break-up/freeze-up metrics used in this study based on Johnson and Eicken (2016) (green shading) and the corresponding dates of ice opening, retreat, advance and closing as defined by Bliss et al. (2019) (yellow shading). A violin plot shows a distribution by widening the horizontal lines in the ranges (of day of the year, in this case) having the highest concentration of values. The thin black lines represent the observations themselves; the black strips are clusters of lines representing groups of

similar values in the distribution. The violin plots provide no information about the temporal sequence of the values.

Deleted: ¶

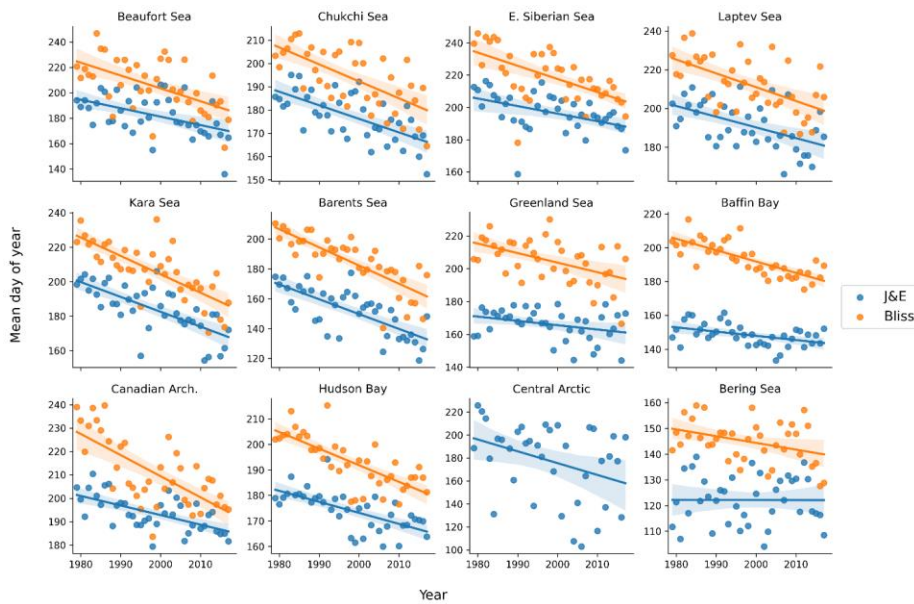


Figure 5. Yearly values of J&E’s break-up end date (blue symbols) and the Bliss et al.’s (2019) Day of retreat (orange symbols) in the various MASIE regions. Corresponding trend lines are shown in each panel. (For the Central Arctic region, the Bliss metric (Day of retreat) was not defined for a sufficient number of years). Y-axis labels represent day of the year. Date scales on y-axis vary among panels in order to optimize display of data points. Numerical values of slopes and their significance levels are provided in Table S2.

Deleted: ¶

Commented [MAJ15]: Added this, same as in Figure 8.

Deleted:

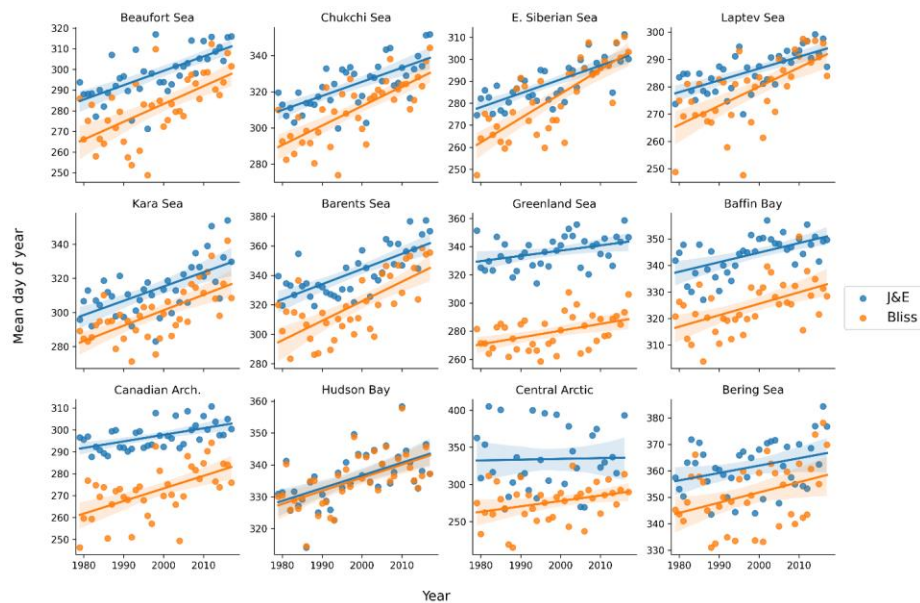


Figure 6. Yearly values of J&E’s freeze-up end date (blue symbols) and the Bliss et al.’s (2019) Day of closing (orange symbols) in the various MASIE regions. Corresponding trend lines are shown in each panel. Y-axes labels represent day of the year. Date scales on y-axis vary among panels in order to optimize display of data points. Numerical values of slopes and their significance levels are provided in Table S3.

Deleted: are Julian dates.

Commented [MAJ16]: From Fig 8.

A final comparison is presented in Figure 7, which shows the ice season lengths computed using the two sets of metrics. The ice season length is defined as the number of days between the end of freeze-up and the start of break-up. Consistent with J&E’s earlier break-up (Figure 5) and later freeze-up (Figure 6), the J&E metrics yield a shorter ice season than the Bliss et al metrics. The differences in Figure 7 exceed a month in most of the Arctic except for the

Deleted: length is generally longer when computed from the J&E metrics

Bering Sea, Hudson Bay and the Canadian Archipelago. However, the negative trends of ice season length are similar in magnitude according to both sets of metrics over most of the Arctic. The trend maps are not shown here because they add little to the information conveyed in Figures 5 and 6.

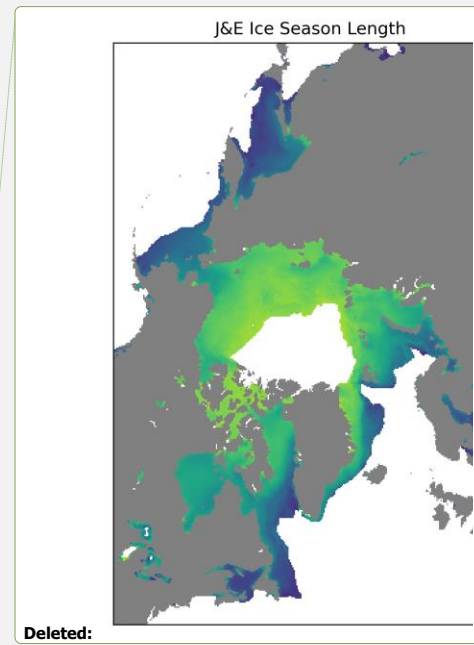
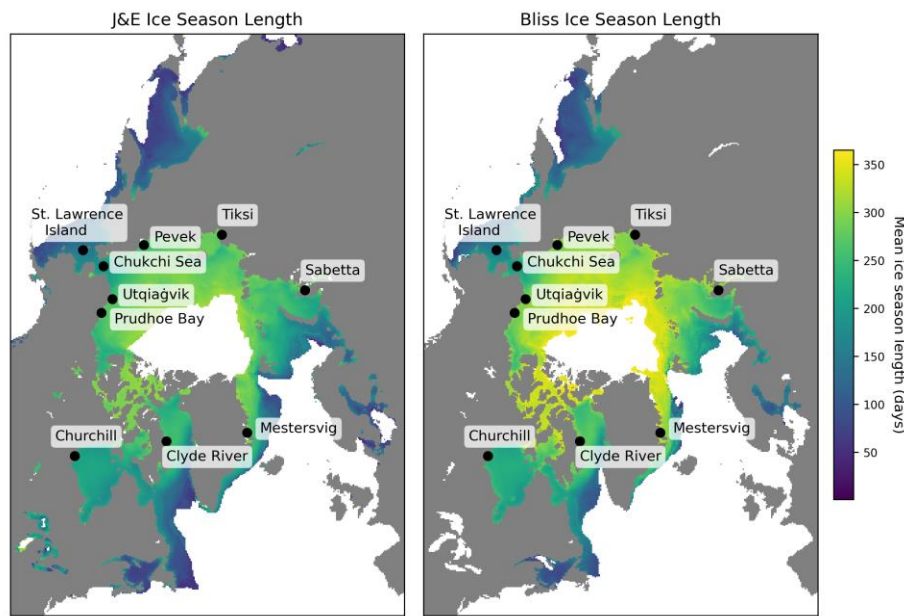


Figure 7. Mean ice season length based on the J&E metrics (left) and the Bliss et al. (2019) metrics (right). Metrics of break-up and freeze-up were not defined in a sufficient number of years in the white area near the North Pole.

Given that the development of local indicators is a main objective of this study, it is important to assess the relationship between the local indicators and those for the broader MASIE regions containing the coastal locations. Figures 8-11 provide these comparisons for all four

Formatted: Space After: 18 pt

Deleted: ¶

Deleted: The main focus of the present study is

Deleted: indicators for the coastal locations

metrics defined by the modified J&E algorithms. In all cases, the yearly values (and linear trend lines) for the ten coastal locations in Table 3 are plotted for the 1979-2018 period, together with the values for the corresponding MASIE regions.

Deleted: 2

The break-up start dates (Figure 8) differ between the coastal locations and the broader MASIE regions in most of the ten cases, and in some cases the trends are notably different. With regard to systematic differences, not only the magnitude but also the sign of the offsets varies among the regions. The break-up start date at the coast is later than for the MASIE regions for Prudhoe (Beaufort Sea), Utqiaġvik (Chukchi Sea), Tiksi (Laptev Sea), and both Canadian locations: Churchill (Hudson Bay) and Clyde River (Baffin Bay). These sites are all Arctic coastal locations at which varying extents of landfast ice are present. By contrast, the coastal locations have earlier break-up start dates (relative to their corresponding MASIE regions) at St. Lawrence Island (Bering Sea), Mestersvig (Greenland Sea) and the Bering Strait (Chukchi Sea). These locations are less prone to experience a buildup of landfast ice during the winter. The results imply that landfast ice [plays a role in](#) the timing of the start of breakup at coastal locations relative to the broader sector of the seasonal sea ice zone. [The processes by which landfast ice affects the timing of break-up are discussed in Section 4.](#)

Deleted: is a key determinant of

Deleted: relative

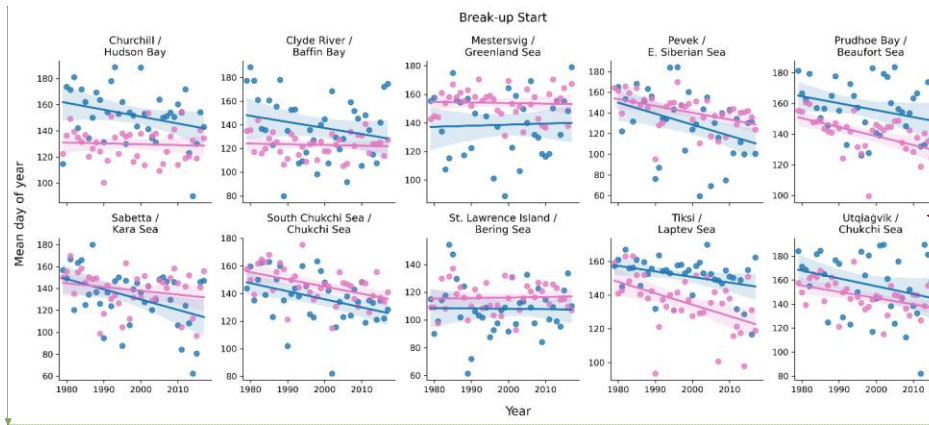
While the general trend towards earlier break-up noted above (Figure 5) is apparent at most of the coastal locations, the magnitudes of the trends can differ between the coastal sites and the broader MASIE regions. Figure 8 shows that ~~the~~ trend towards an earlier start of break-up is stronger at the coastal location relative to the MASIE region at Churchill, Clyde River, Pevek and Sabetta. ~~Only~~ at Tiksi is the negative trend weaker at the coastal site. In the other regions the trends are nearly identical.

Commented [MAJ17]: You don't mean "in most cases" because you define the 4 sites in this sentence where the trend is stronger.

Deleted: , in most cases,

Formatted: Strikethrough

Deleted:



Deleted: The break-up end dates (Figure 9) show differences similar to those in Figure 8 in most, but not all, cases. The break-up end date occurs earlier at Clyde River, Prudhoe and Utqiagvik relative to the MASIE regions, as is the case with the results in Figure 8. However, unlike the break-up start date, the break-up end date also occurs earlier at Mestersvig than for the Greenland Sea MASIE region. The opposite relationship is found in the Kara Sea (Sabetta) and the South Chukchi Sea (Bering Strait), where the MASIE region has the earlier break-up end date. The temporal trends in the break-up end dates are generally similar for the coastal locations and the MASIE regions, and there are no differences in sign. All coastal locations and all MASIE regions show negative trends, i.e., trends toward earlier break-up end dates in recent decades. ¶

Formatted: Right: -0.63" ¶

Figure 8. Yearly values (1979-2018) of the break-up start dates (shown as day-of-the-year numbers)

Deleted: ¶

for the coastal locations (blue) and the corresponding MASIE regions (purple). Date scales on y-axis vary among panels in order to optimize display of data points. Linear regression lines are shown with the same color coding. In each panel, the upper line of header identifies the coastal location and the lower line identifies the MASIE region. All values are based on the modified J&E algorithms. Slopes and their significance levels are listed in Tables S2 and S3.

The break-up end dates (Figure 9) show differences similar to those in Figure 8 in most, but not all, cases. The break-up end date occurs earlier at Clyde River, Prudhoe and Utqiagvik relative to the MASIE regions, as is the case with the results in Figure 8. However, unlike the break-up start date, the break-up end date also occurs earlier at Mestersvig than for the Greenland Sea MASIE region. The opposite relationship is found in the Kara Sea / Sabetta and the Chukchi Sea (Bering Strait), where the MASIE region has the earlier break-up end date. The temporal trends in the break-up end dates are generally similar for the coastal locations and the MASIE regions, and there are no differences in sign. All coastal locations

Commented [MAJ19]: It is a picky point, but you could write "Kara Sea / Sabetta" for consistency with the headers on the figures. Here and for following similar notation, i.e. use "/" ...

and all MASIE regions show negative trends, i.e., trends toward earlier break-up end dates in recent decades.

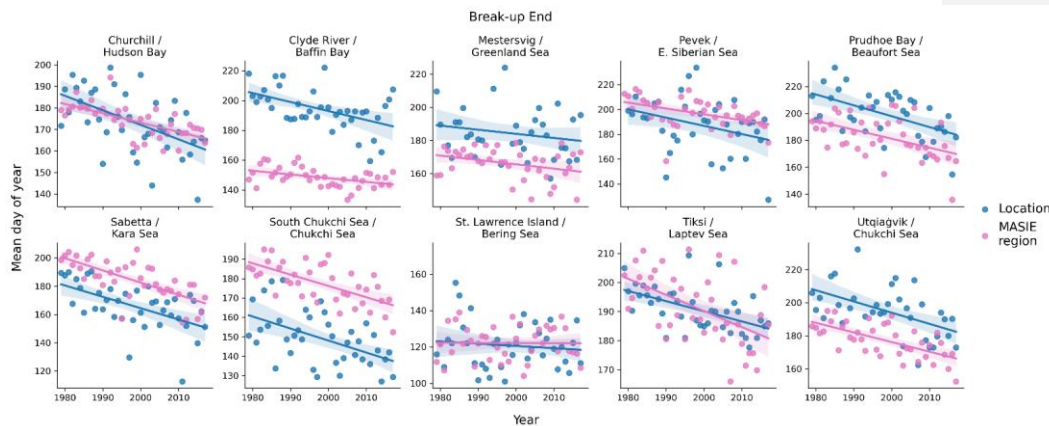


Figure 9. Yearly values (1979-2018) of the break-up end dates (shown as day-of-the-year numbers) for the coastal locations (blue) and the corresponding MASIE regions (purple). Date scales on y-axis vary among panels in order to optimize display of data points. Linear regression lines are shown with the same color coding. In each panel, the upper line of header identifies the coastal location and the lower line identifies the MASIE region. All values are based on the modified J&E algorithms. Slopes and their significance levels are listed in Tables S2 and S3.

The freeze-up start dates are compared in Figure 10. Several regions show large offsets, most notably Clyde River (Baffin Bay) and Mestersvig (Greenland Sea), where the start of freeze-up occurs earlier at the coast by several weeks. Both Baffin Bay and the Greenland Sea are large MASIE regions (Figure 2), favoring the delay of freeze-up start over a substantial portion of the seasonal sea ice zone within the respective MASIE regions. Freeze-up start

Deleted:

Formatted: Space After: 18 pt

Deleted: Same as Figure 8, but for the break-up end dates.

dates are also earlier than offshore at several other coastal locations: Churchill, Sabetta and Utqiaġvik. These are regions in which it is common for ice to form along the coast in autumn, with the ice edge advancing offshore to meet the expanding main ice pack as freeze-up progresses. By contrast, the southern Chukchi Sea location has a later freeze-up date than the Chukchi MASIE region, largely because the southern Chukchi grid cells are located in an area of relatively warm inflowing currents [from the Bering Sea](#) and are in the southern portion of the Chukchi MASIE region. As with the break-up end dates, all coastal locations and MASIE regions show trends of the same sign. In this case, the trends are all positive, indicating a later start to freeze-up.

Finally, Figure 11 compares the freeze-up end dates for the ten coastal sites and their MASIE regions. The results are quite similar to those for the freeze-up start dates in Figure 10. Relative to the MASIE regions as a whole, freeze-up ends earlier at both Canadian sites (Churchill and Clyde River), Mestersvig, Sabetta and Utqiaġvik. Again, the differences are especially large (more than a month) at Clyde River and Mestersvig, both of which are in large MASIE regions as noted above. The southern Chukchi Sea and, to a lesser extent in recent decades, Pevek (East Siberian Sea) show later freeze-ups near the coast than for the MASIE region. Once again, all trends are positive, pointing to a later end to freeze-up at coastal as well as offshore regions throughout the Arctic. The changes in the freeze-up dates over the 40-year period are especially large, exceeding one month, at Pevek (East Siberian Sea) and Prudhoe (Beaufort Sea). The changes are close to a month at Utqiaġvik (Chukchi Sea) and the Southern Chukchi Sea.

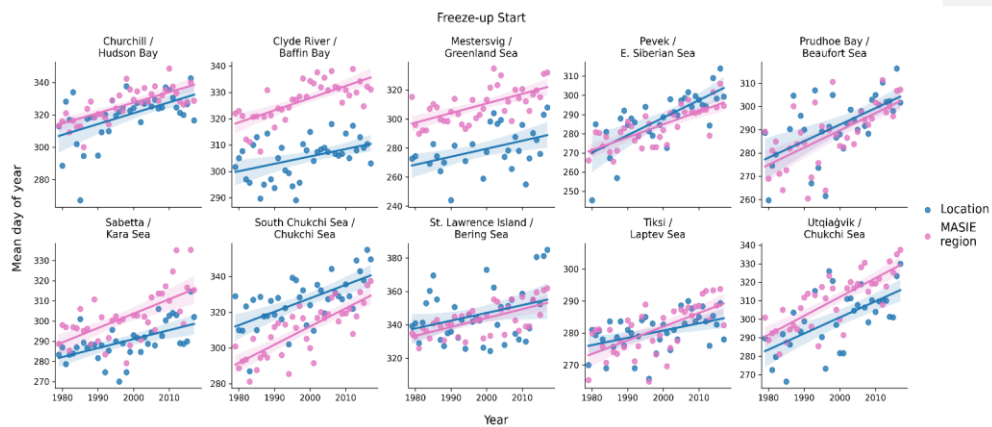


Figure 10. Yearly values (1979-2018) of the freeze-up start dates (shown as day-of-the-year numbers) for the coastal locations (blue) and the corresponding MASIE regions (purple). Date scales on y-axis vary among panels in order to optimize display of data points. Linear regression lines are shown with the same color coding. In each panel, the upper line of header identifies the coastal location and the lower line identifies the MASIE region. All values are based on the modified J&E algorithms. Slopes and their significance levels are listed in Tables S2 and S3.

Deleted:

Deleted: Same as Figure 8, but for the freeze-up start dates.

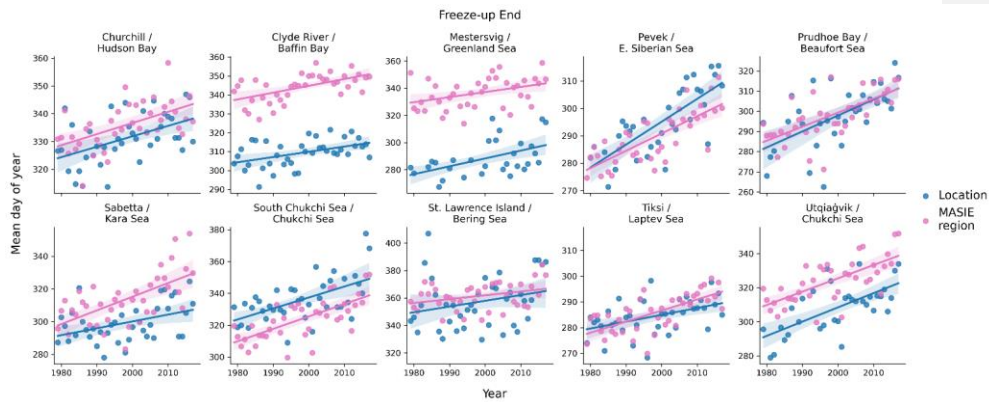


Figure 11. Yearly values (1979-2018) of the freeze-up dates (shown as day-of-the-year numbers) for the coastal locations (blue) and the corresponding MASIE regions (purple). Date scales on y-axis vary among panels in order to optimize display of data points. Linear regression lines are shown with the same color coding. In each panel, the upper line of header identifies the coastal location and the lower line identifies the MASIE region. All values are based on the modified J&E algorithms. Slopes and their significance levels are listed in Tables S2 and S3.

In order to synthesize the information provided by the local indicators, we applied a factor analysis to each of the four local indicators described in Section 2. For the local indicators, each input matrix was 10 (locations) x 40 (years). For comparison, we also applied the factor analysis to the corresponding regional sea ice areas from the MASIE database (National Snow and Ice Data Center dataset G02135_v3.0-4). Because the Chukchi Sea is the MASIE region for two of the local indicators (Chukchi Sea and Utqiagvik), the data matrix for the MASIE regional factor analysis contained 9 (regions) x 40 (years) entries. We performed the MASIE

Deleted:
Formatted: Space After: 24 pt

Deleted: Same as Figure 8, but for the freeze-up end dates.

Deleted: South
Deleted: Utqiagvik

factors separately for middle months of the break-up and freeze-up seasons (June and November, respectively).

In all cases, the first factor contains loadings of the same sign for all locations/regions and is essentially a depiction of the temporal trends, which account for substantial percentages of the variance. The second factor consists of loadings of both signs, corresponding to positive departures from the mean at some locations and negative departures at others. Figure 12 illustrates this behavior for (a) the break-up start dates and (b) the freeze-up end dates. While every one of the ten locations has a positive loading in Factor 1, the mixed signs of the Factor 2 loadings point to a regional clustering of the dates. For example, Figure 12a shows that the northern coastal sites in the Pacific hemisphere (Prudhoe Bay, Utqiagvik, Tiksi, Pevek) have a component of break-up start date variability that is out of phase with the locations in the western Atlantic/eastern Canada sector (Mestersvig, Churchill, Clyde River).

The interpretation of Factor 1 as a trend mode is supported by Figure 13, which shows the time series of the scores of Factor 1 for (a) the break-up start date and (b) freeze-up end dates. The trends towards an earlier start of break-up and a later end of freeze-up are clearly evident. Figure 13 also illustrates the tendency for occasional “outlier” years to be followed by a recovery in the following year. These plots and those for the other local indicators show that these extreme excursions and recoveries are superimposed on the strong underlying trends, resulting in new extremes when the sign of an extreme year is the same as the sign of the underlying trend.

Deleted: 12

Deleted: 12

Commented [MAJ20]: This is interesting. Is this true for planetary climate trends as well??? I did not know this. It means then, for example, SIC “mins” are more extreme as the SIC trend falls in the long term, at the global scale. And “hot” days are hotter as the planet warms. Is my assessment generally correct?

Commented [JWJ21R20]: If the variance does not change, then the statement should be true of any time series – a trend (of either sign) will result in new extremes (of the same sign) if the trend continues long enough.

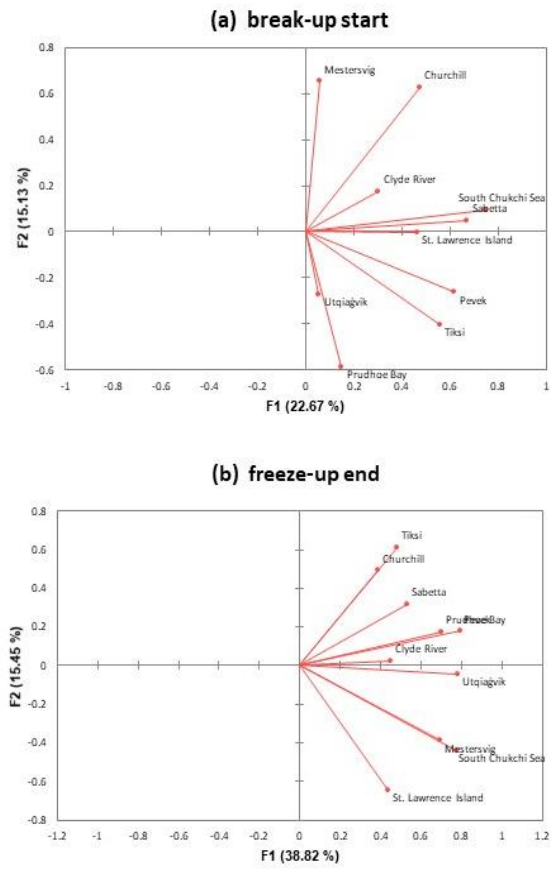


Figure 12. Loadings for Factor 1 (x-axis) and Factor 2 (y-axis) for (a) the start of break-up and (b) the end of freeze-up at the ten local coastal sites. Labels on vectors denote locations.

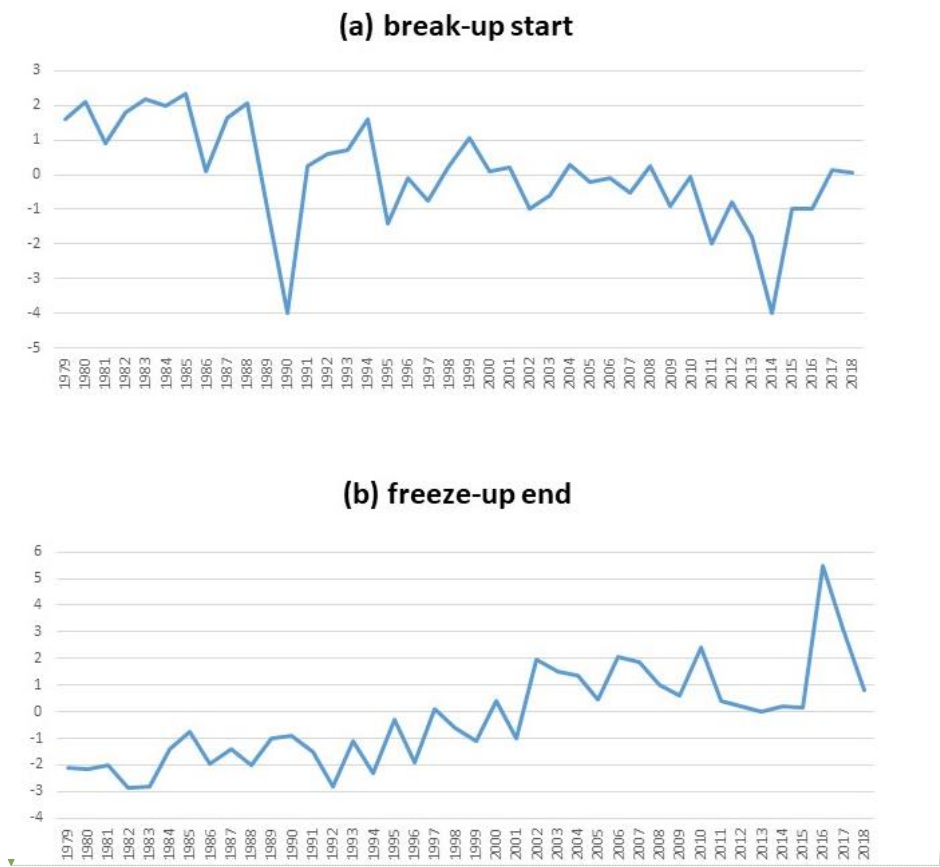
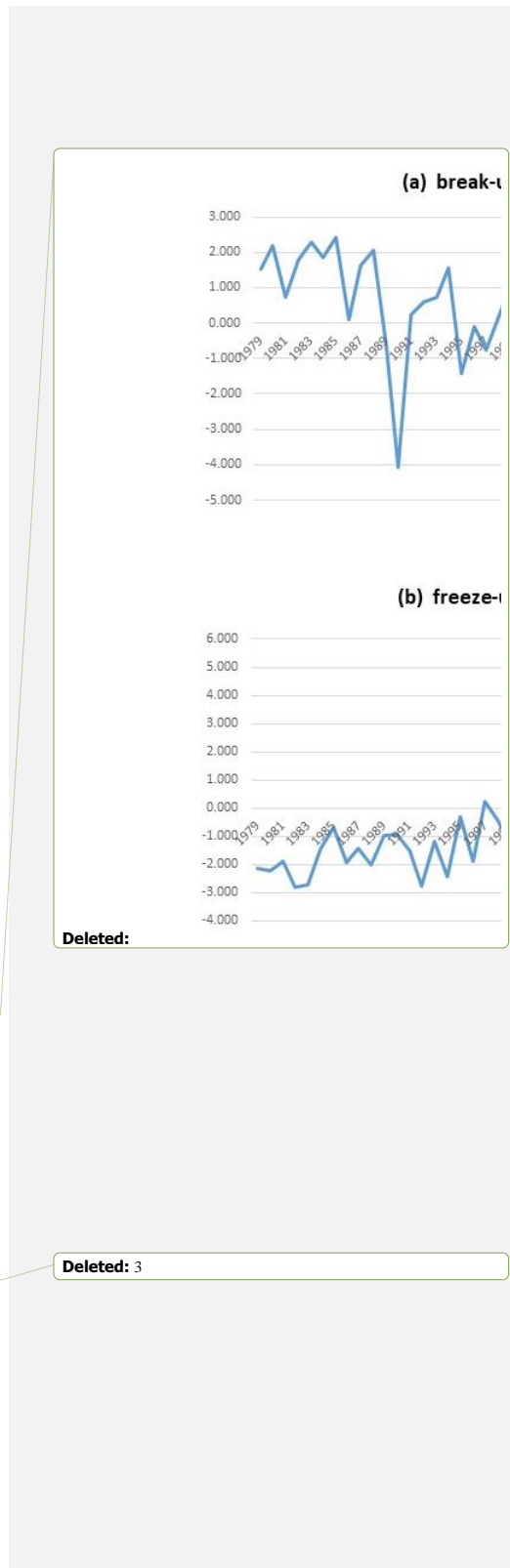


Figure 13. Scores (time series) for Factor 1 of (a) the start of break-up and (b) the end of freeze-up at the ten local coastal sites.

Table 4 shows that the first two factors explained more than half the variance for all local and MASIE indicators except the local break-up start date. The break-up start date is notable for the small percentages of variance explained by the first two factors. The implication is that



local conditions play a relatively greater role in the timing of the start of break-up. These local factors can include landfast ice, inflow of water and heat from the adjacent land areas (including rivers), and possibly other effects related to local ocean currents or local weather conditions. The freeze-up start date has the most spatial coherence in the trend mode (55.7% of the explained variance). However, as shown by the last two lines of Table 4, the MASIE regional ice areas have even greater percentages of variance explained by the first two factors. In both the break-up and freeze-up seasons (June and November), the first two factors explain more than 60% of the variance (vs. 37.8%-55.7% for the local indicators). Because the variance of the ice concentrations in the MASIE regions is generally greater in the southern compared to the northern portion of the region, factors for individual MASIE regions have greater loadings in the south. However, this does not provide an obvious explanation for why the percentage of variance explained by the first factor is greater for the MASIE indicators than for the local indicators. These differences again point to the importance of local conditions relative to the broader underlying trend in ice coverage, as Factor 1 (the trend) accounts for most of the differences between the local and regional results in Table 4.

Table 4. Percentages of variance explained by Factors 1 and 2. Numbers in parentheses are the contributions of the individual factors (Factor 1 + Factor 2).

Break-up start (local)	37.8%	(22.7% + 15.1%)
Break-up end (local)	50.9%	(37.6% + 13.3%)
Freeze-up start (local)	55.7%	(40.1% + 15.6%)
Freeze-up end (local)	54.3%	(38.8% + 15.5%)

Deleted: 3

Deleted: s

Deleted: 3

Deleted: ¶

Deleted: 3

Deleted: start

Deleted:

Deleted:

Deleted:

MASIE ice areas: June	60.9%	(47.1% + 13.8%)
MASIE ice areas: November	64.1%	(48.7% + 15.4%)

Finally, Figure 14 illustrates the tendency for tighter clustering in the regional indicators. For both the June and November results, the clustering in Figure 14 is clearly more distinct than in Figure 12, which is the corresponding figure for the local indicators. The clustering in Figure 14 is geographically coherent, e.g., the Pacific sector sites (Bering, Chukchi, East Siberian) are in a distinct cluster for the June (break-up), while subclusters for November include the Hudson and Baffin regions, the Kara and Laptev regions, and the Bering and Chukchi regions. The results imply that underlying trends and spatially coherent patterns of forcing will be more useful in explaining – and ultimately predicting – variations of regional sea ice cover. However, diagnosis and prediction of local indicators will require a greater reliance on additional information, such as local geography and local knowledge, including information from residents and other stakeholders who have had experience with break-up and freeze-up of sea ice in the immediate area.

Deleted: ¶

Deleted: December

Deleted: (

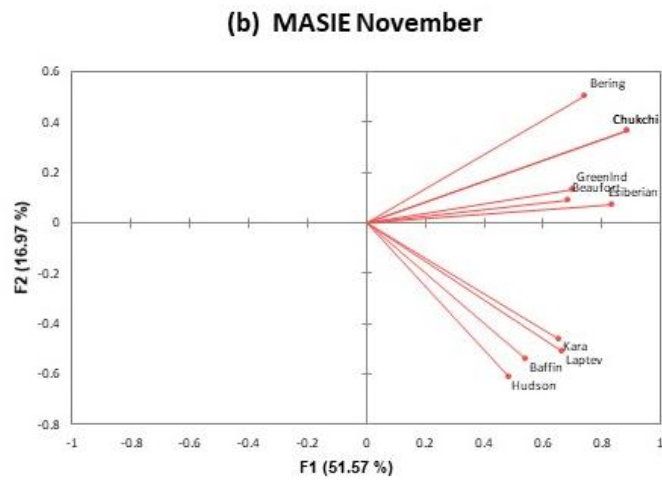
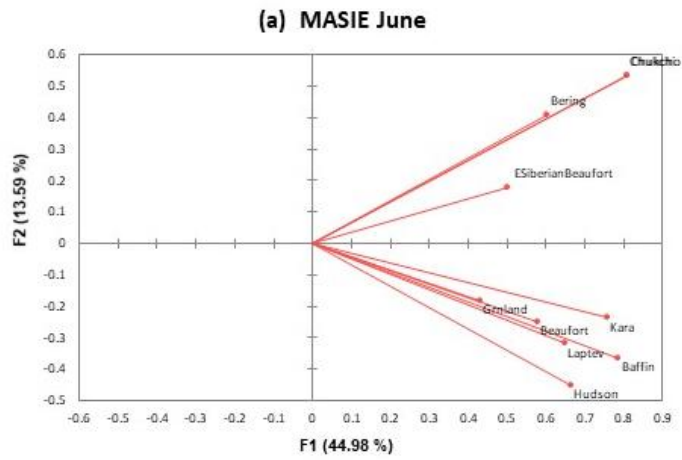


Figure 14. Loadings for Factor 1 (x-axis) and Factor 2 (y-axis) for the MASIE regional ice areas of (a) June and (b) November. Labels on vectors denote MASIE regiona.

4. Discussion

The results presented in Section 3 point to a lengthening of the open water season as a result of both an earlier break-up and a later freeze-up. The timing of break-up and freeze-up relates to the proximity to the coast. In this section, we first place the trends obtained here in the context of past studies. We then address the distinct characteristics of the near-coastal waters by discussing landfast ice and its role in break-up and freeze-up, again drawing upon the published literature for context.

The lengthening of the open-water season in the Arctic has been well-documented (e.g., Stroeve et al., 2014; Stroeve and Notz, 2018; Onarheim et al., 2018; Bliss and Anderson, 2018; Peng et al., 2019; Smith and Jahn, 2019). As a result, the percentage of the Arctic sea ice cover experiencing break-up and freeze-up (i.e., the percentage of the maximum ice cover that is seasonal) has increased from about 50% in 1980 to more than 70% in recent years (Druckenmiller et al., 2021; Thomson et al., 2022). Since 1980, the length of the open water period has increased by between one and two months (over 10 days per decade) (Stammerjohn et al., 2012; Peng et al., 2019; Thomson et al., 2022), with contributions of comparable magnitude from earlier break-up and later freeze-up. Regional variations of these trends, both in the vicinity of the coasts and in regions farther offshore, are the focus of this paper as well as Bliss et al. (2019), to which we have compared our results.

Trends in freeze-up have been shown previously to be sensitive to the criterion for freeze-up (Peng et al., 2018; Bliss et al., 2019). For example, Peng et al. (2018) found that the trends in the autumn crossing of the 80% concentration were greater than trends in the crossing of the 15% threshold (Thomson et al., 2022), implying a slowing of the autumn/winter ice advance.

Deleted: Conclusion

Formatted: Font: (Default) Times New Roman, 12 pt

Formatted: Normal, No bullets or numbering

Deleted: o

Deleted: .

Such findings, as well as those of Johnson and Eicken (2016), have motivated our use of separate indicators for the start and end of break-up and freeze-up.

The delayed autumn freeze-up is a manifestation of the release of increased amounts of heat stored in the upper layers of the ocean, largely as a result of the increased solar absorption made possible by the earlier break-up. In this respect, trends in break-up and freeze-up are intertwined. This linkage has been demonstrated quantitatively by Serreze et al. (2016) and Stroeve et al. (2016), who explored the use of break-up timing as a predictor of the timing of ice advance in the Chukchi Sea and the broader Arctic, respectively.

The results in Section 3 show that the timing of break-up differs at coastal and offshore locations. In most cases, these differences can be related to the presence of landfast ice, which characterizes the nearshore coastal waters to varying degrees at most of our coastal sites.

Figure 15 shows the median and maximum extent of landfast ice during June for the period 1972-2007. Landfast ice is most extensive over shallow waters of the Siberian Seas and the Canadian Archipelago, although it can develop in the general vicinity of all of our sites (Fig. 1), with the exception of the offshore location in the Chukchi Sea. Given its widespread presence at the coastal sites in the Arctic, landfast ice a key feature in our assessment of coastal-offshore differences in particular for ice break-up. It is for this reason that we have attempted to place our findings into a context of landfast ice.

Formatted: Normal, No bullets or numbering

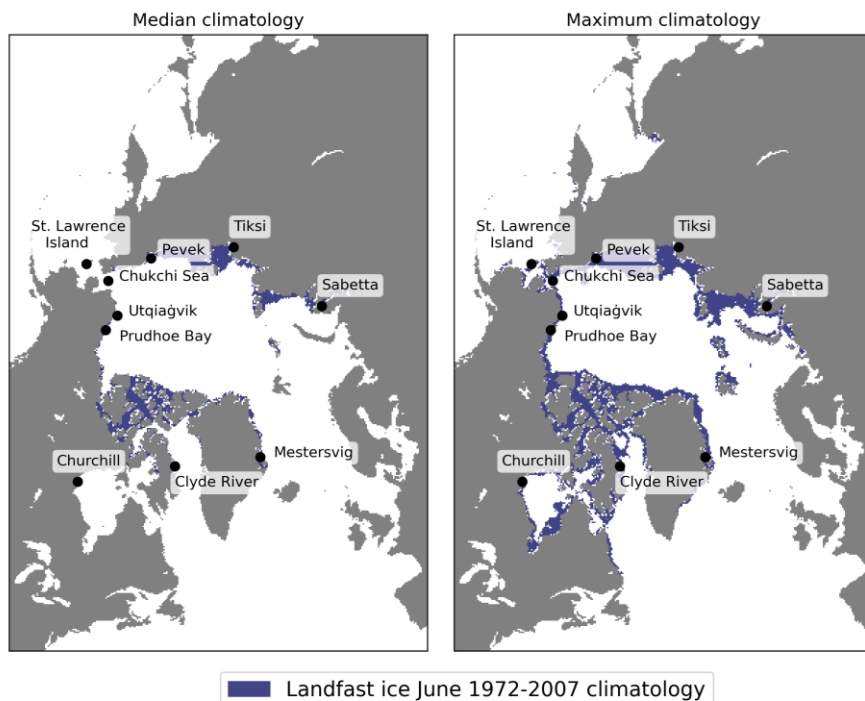


Figure 15. Landfast ice climatology for June based on the digitized ice charts of the National Ice Center. Blue shading denotes median extent (left panel) and maximum extent (right panel) of landfast ice over the 1972-2007 period. Data source: National Ice Center via National Snow and Ice Data Center, NSIDC dataset G02172 -- <https://nsidc.org/data/G02172> (accessed 28 June 2022).

Landfast ice generally persists longer than pack ice in the adjacent offshore in spring. This contrast can be explained largely in terms of the stationary nature of the landfast ice cover, with grounded pressure ridges and confinement by coastal barrier islands (e.g., in the Beaufort and Kara Seas) locking the ice cover in place. Differences in ice thickness, with offshore sea

Formatted: Right: 0"

Deleted: in the

Formatted: Line spacing: Double

Formatted: No underline

ice younger and hence thinner in areas of coastal polynyas with winter new-ice formation (e.g., in the Chukchi, Beaufort and Laptev Seas) may also contribute to longer persistence of landfast ice. Finally, with thermal decay of sea ice as a key break-up mode, the absorption of solar shortwave energy in leads and openings in the offshore ice pack promotes thinning and decay of the offshore ice relative to that of the landfast ice. The latter is mostly lacking such areas of open water, rendering lateral melt and ocean-to-ice heat transfer from subsurface ocean heat storage less effective (see also Petrich et al., 2012).

For coastal sites situated partly or wholly within a landfast ice zone, the breakup dates described in Section 3 are highly dependent on the break-up of the landfast ice. Petrich et al. (2012) describe two dominant break-up modes for landfast ice. Dynamic or mechanical break-up occurs when the action of the wind, ocean swell or currents, and variations in sealevel height promote weakening of the ice cover, detachment from the seafloor and advection of the ice away from the coast. Thermal breakup results from surface and bottom ablation and internal melt, aided further by formation of surface melt ponds. Dispersion is not required for thermal breakup. As noted by Petrich et al. (2012), the mode of ice breakup is often determined by the extent of grounded pressure ridges.

In the autumn, water in the shallow coastal areas cools more rapidly to the freezing point because there is less stored heat below the surface. Coastal waters can also be fresher than offshore waters because of terrestrial runoff that freshens the nearshore areas during the warm season. Under such conditions both a higher freezing point and reduction of convective overturning promote earlier freeze-up (Dmitrenko et al., 1999). As a result, the autumn freeze-up often proceeds outward from the coast as well as shoreward from the main pack ice (Thomson et al., 2022, their Fig. 4). However, onset of freeze-up – and depending on the

geographic setting and offshore ocean and atmosphere conditions potentially also end of freeze-up – do not correspond with onset of landfast ice formation. In the Chukchi and Beaufort Sea, first appearance of landfast ice may lag freeze onset by a couple of weeks to three months (Mahoney et al., 2014). In more sheltered and less dynamic environments such as the Laptev Sea, inshore landfast ice typically does not form for another couple of weeks after onset of freeze-up and generally takes more than a month to extend further offshore (Selyuzhenok et al., 2015). Hence, freeze-up variability and trends reported in this study are seen as largely independent of landfast ice processes.

Conversely, timing of freeze-up does impact the seasonal evolution of landfast ice. Mahoney et al. (2007) discuss mean climatology of annual landfast ice from 1996-2004, including analyses of the maximum, minimum and mean extents. Notable for the results presented in the present study is Mahoney et al.'s finding of a reduced presence of landfast ice in Beaufort-Chukchi region, due to later formation and earlier breakup. In a follow-up study, Mahoney et al. (2014) addressed the geographical variability of break-up and freeze-up, especially as it relates to landfast ice. Their results show that landfast ice in the central and western Beaufort Sea forms earlier, breaks up later, occupies deeper water and extends further from shore than that in the Chukchi Sea. These differences are partially due to the orientation of the coastline relative to the prevailing easterly winds, which can more readily advect ice away from the southwest-northeast oriented coastline of the Chukchi Sea. Hosekova et al. (2021) examined landfast ice along the northern Alaska coast in the context of the buffering of the coastline from wave activity. They found that the wave attenuation by landfast ice was weaker in autumn than in spring because of the lower ice thickness in autumn compared to spring. However, the importance of waves for breakup is somewhat limited because it typically

Formatted: Comment Text, No bullets or numbering

Commented [HE24]: Not sure whether this is needed here, since it doesn't relate that clearly to timing of the freezeup and breakup. If we keep it, we could add a brief mention that the importance of waves for breakup is somewhat limited because it typically requires large fetch with does not develop until later in the summer and fall, well past the end of break-up season.

Formatted: Font: (Default) Times New Roman, 12 pt

Formatted: Font: (Default) Times New Roman, 12 pt

requires large fetch with does not develop until later in the summer and fall, well past the end of break-up season.

Yu et al. (2014) showed that landfast ice has large interannual variations, which imply large variations in break-up and freeze-up. Superimposed on these variations were notable trends in landfast ice during Yu et al.'s study period, 1976-2007. More specifically, the duration of landfast ice was found to have shortened in the Chukchi, East Siberian and Laptev Seas, primarily as a result of a slower offshore expansion of landfast ice during the autumn and early sinter since 1990. Our coastal sites in these sectors (Utqiagvik, Pevek and Tiksi) show notable trends toward earlier break-up and later freeze-up, consistent with Yu et al.'s (2014) trends in landfast ice.

Cooley et al. (2020) examined the sensitivity of landfast ice break-up at the community level in the Canadian Arctic and western Greenland to temperature variations and trends based on analysis of visible satellite imagery. Our analysis provides a longer reference period (40 years vs. 19 years) and a broader geographical context for the work by Cooley and collaborators. Cooley et al. (2020) also used the relationships between air temperature and landfast ice break-up date, together with projected changes in air temperature from a set of eight CMIP5 global climate models, to project future changes in the breakup dates. Specifically, we note that the trends projected for the remainder of the century in Cooley et al. (2020) are in many instances less pronounced (in days/decade shift in breakup) than those identified here. For example, for Clyde River Cooley et al. project a shift in breakup to an earlier date by 23 days by the year 2099 as compared to changes of a similar magnitude but over a much shorter time period examined here (Fig. 8 and 9). For Clyde River, the comparison between trends in the local break-up timing compared to that for the broader region (Baffin Bay) also reveals that

Formatted: Font: (Default) Times New Roman

Formatted: Line spacing: Double

Formatted: Font: (Default) Times New Roman

Formatted: Font: (Default) Times New Roman

Formatted: Normal (Web), Space After: 12 pt, Line spacing: Double

the regional trends are much less pronounced than those at the local scale (Fig. 8 and 9). Furthermore, the two westernmost communities examined by Cooley et al. (2020), Tuktoyaktuk and Paulatuk (Eastern Beaufort Sea), were projected to see earlier landfast ice break-up onset of 5 days and 11 days, respectively, by 2099. The data compiled here for Prudhoe Bay and the Beaufort Sea indicate a substantially larger shift towards earlier dates by more than 5 days *per decade* (Fig. 8 and 9).

Formatted: Font: Italic

One other study that addressed future changes of sea ice duration in the Pacific sector of the Arctic is Wang et al.'s (2018) evaluation mid-21st-century projections based on sea ice concentrations simulated by seven CMIP5 global climate models. However, Wang et al.'s evaluations were for the broader offshore areas of the East Siberian, Chukchi and Beaufort Seas rather than for immediate coastal areas, as global climate models generally do not include landfast ice. Pan-Arctic models that simulated landfast ice parameterized thermodynamically without addressing its mobility had significant problems in forecasting coastal ice thickness, especially during freeze-up in September and October (Johnson et al., 2012). The projected increases in ice-free season length over the 2015-2044 period were found to vary from about 20 days in the Bering Strait region to up to 60 days in the offshore areas of the East Siberian, Chukchi and Beaufort Seas. While these changes are for offshore areas, they are larger than those projected for coastal areas by late century in the study of Cooley et al. (2020).

Formatted: Normal (Web), Space After: 12 pt, No bullets or numbering

Formatted: Superscript

Deleted: in

5. Conclusion

The primary objective of this study was to use the locally-based metrics to construct indicators of break-up and freeze-up at near-coastal locations in which sea ice has high

Commented [MAJ25]: This seems relevant. If not, or it seems too self-serving, take it out.

Commented [JWJ26R25]: Seems relevant to me.

Moved down [1]: This study has utilized sea ice indicators based on local ice climatologies informed by community ice use (Johnson and Eicken, 2016; Eicken et al., 2014) rather than prescribed "universal" thresholds of ice concentration (e.g., 15%, 80%) used in other recent studies of sea ice break-up and freeze-up.

Deleted: Both types of indicators show similar trends and associated interannual variations, but the more locally-tailored indicators generally show earlier break-up and, in many instances, later freeze-up.

Deleted: indicators

stakeholder relevance. A set of ten coastal locations distributed around the Arctic were selected for this purpose. The sea ice indicators used here are based on local ice climatologies informed by community ice use (Johnson and Eicken, 2016; Eicken et al., 2014) rather than prescribed “universal” thresholds of ice concentration (e.g., 15%, 80%) used in other recent studies of sea ice break-up and freeze-up.

The trends and interannual variations of the local indicators of break-up and freeze-up at the ten nearshore are similar to the trends and variations of corresponding indicators for broader offshore regions, but the site-specific indicators often differ from the regional indicators by several days to several weeks. Relative to indicators for broader adjacent seas, the coastal indicators show later break-up at sites known to have extensive landfast ice, whose break-up typically lags retreat of the adjacent, thinner drifting ice. The coastal indicators also show an earlier freeze-up at some sites in comparison with freeze-up for broader offshore regions, likely tied to earlier freezing of shallow water regions and areas affected by freshwater input from nearby streams and rivers. However, the trends towards earlier break-up and later freeze-up are unmistakable over the post-1979 period at nearly all the coastal sites and their corresponding regional seas.

The differences between the coastal and offshore regional indicators matter greatly to local users whose harvesting of coastal resources and Indigenous culture are closely tied to the timing of key events in the seasonal ice cycle (Huntington et al., 2021; Eicken et al., 2014). These differences also matter from the perspective of maritime activities, where access to coastal locations for destination traffic is a key factor (Brigham, 2017). These offsets vary considerably by region. In light of these findings, we view locally as well as regionally defined measures of sea-ice break-up and freeze-up as a key set of indicators linking pan-

Moved (insertion) [1]

Deleted: is

Deleted: study has utilized

Arctic or global indicators such as sea-ice extent or volume to local and regional uses of sea ice, with the potential to inform community-scale adaptation and response.

Acknowledgments

This work was supported by the Climate Program Office of the National Oceanic and Atmospheric Administration through Grant NA17OAR431060. Additional funding was provided by the Interdisciplinary Research for Arctic Coastal Environments (InterFACE) project through the U.S. Department of Energy, Office of Science, Biological and Environmental Research RGMA program.

Formatted: Space After: 0 pt

Data Availability

The daily grids of passive-microwave-derived sea ice concentrations are available from the National Snow and Ice Data Center as dataset NSIDC-0051, available at <https://nsidc.org/data/nsidc-0051>. Lists of the indicator dates for the coastal sites and the MASIE regions are available from the author on request.

Deleted: ¶

Formatted: Font:

Formatted: Space After: 24 pt

Author contributions

JEW served the principal investigator for the study, led the drafting of the manuscript, and performed the factor analysis described in Section 3. HE supervised the implementation of the revised indicators for the coastal sites and the MASIE regions, and drafted parts of the text. KR performed the indicator calculations, produced Figures 1-11, and assisted in the

Deleted: 4

preparation of the manuscript. MJ designed the original indicators, participated in the modification of the indicators, and contributed to the revision of the manuscript.

Competing interests

The authors declare that they have no conflict of interest

References

AMAP: Adaptation Actions for a Changing Arctic: Perspectives from the Baffin Bay/Davis Strait Region. Arctic Monitoring and Assessment Programme (AMAP), Oslo, Norway. xvi + 354 pp, <https://www.amap.no/documents/download/3015/inline>, 2018.

AMAP: Snow, water, ice and permafrost in the Arctic (SWIPA) 2017, Arctic Monitoring and Assessment Programme (AMAP), Oslo, Norway, xiv + 269 pp. 2017.

Bliss, A.C., and Anderson, M.R.: Arctic sea ice melt onset and timing from passive microwave- and surface air temperature-based methods, *J. Geophys. Res.*, 123, 9063-9080, <https://doi.org/10.1029/2018JD028676>, 2018.

Bliss, A.C., Steele, M., Peng, G., Meier, W.M., and Dickinson, S: Regional variability of Arctic sea ice seasonal climate change indicators from a passive microwave climate data record, *Environ. Res. Lett.*, 14, 045003, <https://doi.org/10.1088/1748-9326/aafb84>, 2019.

Box, J.E., and 19 coauthors: Key indicators of Arctic climate change: 1971–2017, *Environ. Res. Lett.*, 14(4), 045010, <https://doi.org/10.1088/1748-9326/aafc1b>, 2019.

Brigham, L.W.: The changing maritime Arctic and new marine operations. In: Beckman, R. C., Henriksen, T., Dalaker Kraabel, K., Molenaar, E. J., and Roach, J. A. (eds.): *Governance of Arctic shipping* (pp. 1-23), Brill Nijhoff, 2017.

Cavaliere, D.J., Gloersen, P., and Campbell, W.J.: Determination of sea ice parameters with the NIMBUS-7 SMMR, *J. Geophys. Res.*, 89(D4): 5355-5369, <https://doi.org/10.1029/JD089iD04p05355>, 1984.

Cooley, S.W., Ryan, J.C., Smith, L.C., Horvat, C., Pearson, B., Dale, B. and Lynch, A.H.: Coldest Canadian Arctic communities face greatest reductions in shorefast sea ice. *Nature Climate Change*, 10(6), pp.533-538. <https://www.nature.com/articles/s41558-020-0757-5>, 2020.

Formatted: data-table__copy

Formatted: Font: Not Bold

Deleted: ...

Deleted: ,

Deleted: p

Deleted:),

Deleted:

Deleted:

Deleted:

Deleted: Sea

Deleted: Ice

Deleted: Parameters

Formatted: Font: (Default) Times New Roman

Formatted: Font: (Default) Times New Roman

Formatted: Font: (Default) Times New Roman

Formatted: Font: (Default) Times New Roman

Deleted: ¶

Comiso, J. C.: Characteristics of Arctic Winter Sea Ice from Satellite Multispectral Microwave Observations, *J. Geophys. Res.*, 91(C1), 5C0766, 975-994, 1986

Dammann, D.O., Eicken, H., Mahoney, A.R., Meyer, F.J. and Betcher, S: Assessing sea ice trafficability in a changing Arctic. *Arctic*, 71(1), 59-75, <https://doi.org/10.14430/arctic4701>, 2018.

Deser, C., Walsh, J.E., and Timlin, M.S.: Arctic sea ice variability in the context of recent atmospheric circulation trends, *J. Climate*, 13, 617-633, [https://doi.org/10.1175/1520-0442\(2000\)013<0617:ASIVIT>2.0.CO;2](https://doi.org/10.1175/1520-0442(2000)013<0617:ASIVIT>2.0.CO;2), 2000.

Druckenmiller, M.L. et al.: *The Arctic*. *Bull. Amer. Meteor. Soc.*, 102, S263-S316, <https://doi.org/10.1175/BAMS-D-21-0086.1>, 2021.

Eicken, H., Kaufman, M., Krupnik, I., Pulsifer, P., Apangalook, L., Apangalook, P., Weyapuk Jr, W., and Leavitt, J.: A framework and database for community sea ice observations in a changing Arctic: An Alaskan prototype for multiple users, *Polar Geogr.*, 37(1), 5-27, <http://dx.doi.org/10.1080/1088937X.2013.873090>, 2014.

Fang, A., and Wallace, J. M.: Arctic sea ice variability on a timescale of weeks in relation to atmospheric forcing, *J. Climate*, 7, 1897-1914, [https://doi.org/10.1175/1520-0442\(1994\)007<1897:ASIVOA>2.0.CO;2](https://doi.org/10.1175/1520-0442(1994)007<1897:ASIVOA>2.0.CO;2), 1994. .

Fu, D., Liu, B., Yu, G., Huang, H., and Qu, L: Multiscale variations in Arctic sea ice motion and links to atmospheric and oceanic conditions, *The Cryosphere*, 15, 3797-3811, <https://doi.org/10.5194/tc-15-3797-2021>, 2021.

Hosekova, L., Eidam, E., Panteleev, G., Rainville, L., Rogers, W.E., and Thomson, J.: Landfast ice and coastal wave exposure in northern Alaska. *Geophys. Res. Lett.*, 48(22), e2021GL095103, <https://doi.org/10.1029/2021GL095103>, 2021.

Huntington, H. P., Raymond-Yakoubian, J., Noongwook, G., Naylor, N., Harris, C., Harcharek, Q. and Adams, B.: "We never get stuck": A collaborative analysis of change and coastal community subsistence practices in the northern Bering and Chukchi Seas, *Alaska, Arctic*, 74(2), 113-126, 2021.

IPCC: *Climate Change 2021: The Physical Science Basis. Contribution of Working Group I to the Sixth Assessment Report of the Intergovernmental Panel on Climate Change* [Masson-Delmotte, V., Zhai, P., Pirani, A., Connors, S. L., Péan, C., Berger, S., Caud, N., Chen, Y., Goldfarb, L., Gomis, M. I., Huang, M., Leitzell, K. Lonnoy, E., Matthews, J. B. R., Maycock, T. K., Waterfield, Y., Yelekçi, O., Yu, R., and Zho, B. (eds.)]. Intergovernmental Panel on Climate Change, Cambridge University Press. <https://www.bing.com/search?FORM=AFSCVO&PC=AFSC&q=IPCC+AR6+Working+Group+1+report>, 2022.

Johnson, M., and Eicken, H.: Estimating Arctic sea-ice freeze-up and break-up from the satellite record: A comparison of different approaches in the Chukchi and Beaufort Seas,

- Deleted:
- Deleted:
- Deleted:
- Deleted:
- Formatted: No underline
- Field Code Changed
- Formatted: No underline
- Formatted: No underline
- Deleted:
- Deleted:
- Deleted: DOI:
- Formatted: Space After: 8 pt, Line spacing: Multiple 1.08 li
- Formatted: No underline
- Deleted: ¶
- Deleted: ,

Deleted:

Deleted: p.

Deleted: :

Deleted:

Deleted: :

Deleted:

Elementa: Science of the Anthropocene, 4, 000124, doi:10.12952/journal.elementa.000124, 2016.

Johnson, M., et al.: Evaluation of Arctic sea ice thickness simulated by Arctic Ocean Model Intercomparison Project models, J. Geophys. Res., 117, C00D13, doi:10.1029/2011JC007257, 2012

Kapsch, M.L., Eicken, H., and Robards, M.: Sea ice distribution and ice use by indigenous walrus hunters on St. Lawrence Island, Alaska. In SIKU: Knowing Our Ice (Krupnik, I., Aporta, C., Gearheard, S., Laidler, G. J., and Lielsen Holm, L., Eds.), 115-144, Springer, Dordrecht, 2010.

Krupnik, I., Apangalook, L., and Apangalook, P: "It's cold, but not cold enough": Observing ice and climate change in Gambell, Alaska, in IPY 2007-2008 and beyond. In SIKU: Knowing Our Ice (Krupnik, I., Aporta, C., Gearheard, S., Laidler, G. J., and Lielsen Holm, L., Eds.), 81-114, Springer, Dordrecht, 2010.

Mahoney, A.R., Eicken H., Gaylord A.G., and Gens R.: Landfast sea ice extent in the Chukchi and Beaufort Seas: The annual cycle and decadal variability. Cold Reg. Sci. Technol. 103, 41-56. doi: 10.1016/j.coldregions.2014.03.0033, 2014.

Mahoney, A.R., Eicken, H., Gaylord, A.G., and Shapiro, L.: Alaska landfast sea ice: Links with bathymetry and atmospheric circulation, J. Geophys. Res., 112, C02001, doi:10.1029/2006JC003559, 2007.

Markus, T., Stroeve J. C., and Miller, J: Recent changes in Arctic sea ice melt onset, freezeup and melt season length, J. Geophys. Res. (Oceans), 114, 1-14, https://doi.org/10.1029/2009JC005436, 2009.

Meier, W., Fetterer, F., Savoie, M., Mallory, S. Duerr, R., and Stroeve, J.: NOAA/NSIDC Climate Data Record of Passive Microwave Sea Ice Concentration, Version 3 (Boulder, Colorado USA; National Snow and Ice Data Center), https://doi.org/10.7265/N59P2ZTG, [Accessed 16 January 2022], 2017.

Noongwook, G.: Native Village of Savoonga, Native Village of Gambell. In Huntington, H.F., and George, J.C.: Traditional knowledge of the bowhead whale (Balaena mysticetus) around St. Lawrence Island Alaska, 47-54, 2007.

Onarheim, I.H., Eldevik, T., Smedsrud, L.H., and Stroeve, J.C.: Seasonal and regional manifestations of Arctic sea ice loss, J. Climate, 31, 4917-4932, https://doi.org/10.1175/JCLI-D-17-0427.1, 2018.

Peng, G., Steele, M., Bliss, A. C., Meier, W. N., and Dickinson, S: Temporal means and variability of Arctic sea ice melt and freeze season climate indicators using a satellite climate data record, Remote Sensing, 10, 1328, https://doi.org/10.3390/rs10091328, 2018.

Deleted: Elements

Deleted: ¶

Deleted: . (2012),

Deleted:

Formatted: Font: (Default) Times New Roman

Formatted: Font: (Default) Times New Roman

Deleted: .

Formatted: Font: (Default) Times New Roman, 12 pt, Not Bold

Formatted: Font: (Default) Times New Roman, 12 pt, Not Bold

Formatted: Font: (Default) Times New Roman, 12 pt, Not Bold

Formatted: Font: (Default) Times New Roman, 12 pt, Not Bold

Formatted: Font: (Default) Times New Roman, 12 pt, Not Bold

Formatted: Font: (Default) Times New Roman, 12 pt, Not Bold

Formatted: Font: (Default) Times New Roman, 12 pt, Not Bold

Formatted: Font: (Default) Times New Roman, 12 pt, Not Bold

Formatted: Font: (Default) Times New Roman, 12 pt, Not Bold

Formatted: Font: (Default) Times New Roman, 12 pt, Not Bold

Formatted: Font: (Default) Times New Roman, 12 pt, Not Bold

Formatted: Font: (Default) Times New Roman, 12 pt, Not Bold

Formatted: Font: (Default) Times New Roman, 12 pt, Not Bold

Formatted: Font: (Default) Times New Roman, 12 pt, Not Bold

Formatted: Font: (Default) Times New Roman, Not Bold

Formatted: Font: (Default) Times New Roman, Not Bold

Formatted: Font: (Default) Times New Roman, Not Bold

Formatted: Font: (Default) Times New Roman, Not Bold

Formatted: Font: (Default) Times New Roman, Not Bold

Deleted: ¶

Deleted: freezeuo

Deleted:]

Formatted: No underline

Petrich, C., Eicken, H., Zhang, J., Krieger, J., Fukamachi, Y. and Ohshima, K.J.: Coastal landfast sea ice decay and breakup in northern Alaska: Key processes and seasonal prediction, *J. Geophys. Res.*, 117, C02003, doi:10.1029/2011JC007339, 2012.

Formatted: Font: (Default) Times New Roman, Not Bold

Formatted: Normal (Web)

Formatted

Selyuzhenok, V., Krumpfen, T., Mahoney, A., Janout, M., and Gerdes, R.: Seasonal and interannual variability of fast ice extent in the southeastern Laptev Sea between 1999 and 2013, *J. Geophys. Res. Oceans*, 120, 7791–7806, doi:10.1002/2015JC011135, 2015.

Smith, A., and Jahn, A.: Definition differences and internal variability affect the simulated Arctic sea ice melt season, *The Cryosphere*, 12, 1-20, <https://doi.org/10.5194/tc-13-1-2019>, 2019.

Serreze, M.C., Crawford, A.D., Stroeve, J.C., Barrett, A.P. and Woodgate, R.A.: Variability, trends, and predictability of seasonal sea ice retreat and advance in the Chukchi Sea. *J. Geophys. Res. (Oceans)*, 127, 7308–7325, 2016.

Formatted

Stammerjohn, S., Massom, R., Rind, D. and Martinson, D.: Regions of rapid sea ice change: an inter-hemispheric seasonal comparison. *Geophys. Res. Lett.*, 39, L06501, 2017.

Formatted

Stroeve, J.C., Crawford, A.D. and Stammerjohn, S.: Using timing of ice retreat to predict timing of fall freeze-up in the Arctic. *Geophys. Res. Lett.*, 43, 6332–6340, 2016.

Formatted

Stroeve, J.C., Markus, T., Boisvert, L., Miller, J., and Barrett, A.: Changes in Arctic melt season and implications for sea ice loss. *Geophys. Res. Lett.*, 41, 1216-1225, <https://doi.org/10.1002/2013GL058951>, 2014.

Formatted: No underline

Stroeve, J., and Notz, D.: Changing state of Arctic sea ice across all seasons. *Env. Res. Lett.*, 13, 102001, <https://doi.org/10.1088/1748-9326/aade56>, 2018.

Formatted: No underline

Thomson, J., Smith, M., Drushka, K. and Lee, C.: Air-ice-ocean interactions and the delay of autumn freeze-up in the western Arctic Ocean. *Oceanography*, <https://doi.org/10.5670/oceanog.22.124>, 2022.

Formatted: Font: Italic

Formatted: No underline

USGCRP: Climate Science Special Report: Fourth National Climate Assessment, Volume I (Wuebbles, D.J., Fahey, D.W., Hibbard, K.A., Dokken, D.J., Stewart, B.C., and Maycock, T.K.[eds.]). U.S. Global Change Research Program, Washington, DC, USA, 470 pp., doi: 10.7930/JOJ964J6, 2017.

Formatted

Wang, M., Yang, Q., Overland, J.E., and Stabeno, P.: Sea-ice cover timing in the Pacific Arctic: The present and projections to mid-century by selected CMIP5 models. *Deep Sea Research Part II: Topical Studies in Oceanography*, 152, 22-34, <https://www.sciencedirect.com/science/article/pii/S0967064516302132>, 2018

Deleted: ¶

Formatted: Font: (Default) Times New Roman

Formatted: Line spacing: single

Formatted

Walsh, J. E., and Johnson, C. M.: Interannual atmospheric variability and associated fluctuations in Arctic sea ice extent, *J. Geophys. Res.*, 84, 6915–6928, <https://doi.org/10.1029/JC084iC11p06915>, 1979.

Formatted: Space After: 12 pt

Yu, Y, Stern, H., Fowler, C., Fetterer, F., and Maslanik, J.: Interannual variability of Arctic landfast ice between 1976 and 2007. *J. Climate*, Vol. 27, 227-243, doi: 10.1175/JCLI-D-13-00178.1, 2014.

Formatted: Font: (Default) Times New Roman, 12 pt, Not Bold

Formatted: Font: (Default) Times New Roman, 12 pt, Not Bold

Formatted: Font: (Default) Times New Roman, 12 pt, Not Bold

Formatted: Font: (Default) Times New Roman, 12 pt, Not Bold

Formatted: Font: (Default) Times New Roman, 12 pt, Not Bold

Formatted: Font: (Default) Times New Roman, 12 pt, Not Bold

Formatted: Font: (Default) Times New Roman, 12 pt, Not Bold

Formatted: Font: (Default) Times New Roman, 12 pt

Supplementary material

Table S1. Dates (Julian day numbers) corresponding to the modal values (peaks) of the distributions in Figure 4. (Insufficient number of years met Bliss criteria in Central Arctic).

	Break-up Start		Break-up end		Freeze-up start		Freeze-up end	
	J&E	Bliss	J&E	Bliss	J&E	Bliss	J&R	Bliss
Beaufort Sea	145	187	167	208	292	287	296	279
Chukchi Sea	147	177	181	202	315	312	325	302
E. Sibarian Sea	150	182	195	207	281	293	280	294
Laptev Sea	140	192	188	207	280	271	285	279
Kara Sea	145	193	190	209	304	299	307	296
Barents Sea	146	164	152	186	315	297	328	302
Greenland Sea	150	177	162	207	308	290	342	280
Baffin Bay	121	152	149	186	331	311	346	324
Canadian Arctic	147	208	190	207	279	274	298	275
Hudson Bay	139	159	177	198	322	317	326	325
Central Arctic	199		200		306		310	
Bering Sea	110	123	123	142	343	337	362	349

Deleted: ¶

Formatted: Font: (Default) Times New Roman, 12 pt, Bold

Formatted: Font: Bold

Formatted: Indent: Left: 0", Hanging: 0.75", Tab stops: 0.69", Left + 0.75", Left

Formatted: Font: Not Bold

Table S2. Slopes (least-squares linear regression lines) of the MASIE regions in Figures 5-6 and 8-11. Also shown are the explained variances (r^2 values of the trend lines and their levels of statistical significance.

Formatted: Superscript

Region	Indicator Group	Indicator	Slope (days yr ⁻¹)	r ²	significance level
Baffin Bay	Bliss	Day of Advance	0.4	0.57	< 0.01**
Baffin Bay	Bliss	Day of Closing	0.4	0.52	< 0.01**
Baffin Bay	Bliss	Day of Opening	-0.5	-0.74	< 0.01**
Baffin Bay	Bliss	Day of Retreat	-0.7	-0.77	< 0.01**
Baffin Bay	J&E	Break-up End	-0.2	-0.44	< 0.01**
Baffin Bay	J&E	Break-up Start	-0.1	-0.07	0.67
Baffin Bay	J&E	Freeze-up End	0.4	0.57	< 0.01**
Baffin Bay	J&E	Freeze-up Start	0.5	0.71	< 0.01**
Barents Sea	Bliss	Day of Advance	1.3	0.7	< 0.01**
Barents Sea	Bliss	Day of Closing	1.3	0.7	< 0.01**
Barents Sea	Bliss	Day of Opening	-1.1	-0.72	< 0.01**
Barents Sea	Bliss	Day of Retreat	-1.2	-0.79	< 0.01**
Barents Sea	J&E	Break-up End	-1.0	-0.72	< 0.01**
Barents Sea	J&E	Break-up Start	-0.4	-0.38	0.02*
Barents Sea	J&E	Freeze-up End	1.0	0.72	< 0.01**
Barents Sea	J&E	Freeze-up Start	1.0	0.8	< 0.01**
Beaufort Sea	Bliss	Day of Advance	0.8	0.61	< 0.01**
Beaufort Sea	Bliss	Day of Closing	0.9	0.63	< 0.01**
Beaufort Sea	Bliss	Day of Opening	-0.7	-0.51	< 0.01**
Beaufort Sea	Bliss	Day of Retreat	-1.0	-0.56	< 0.01**
Beaufort Sea	J&E	Break-up End	-0.7	-0.48	< 0.01**
Beaufort Sea	J&E	Break-up Start	-0.6	-0.51	< 0.01**

Formatted Table

Beaufort Sea	J&E	Freeze-up End	0.7	0.68	< 0.01**
Beaufort Sea	J&E	Freeze-up Start	0.7	0.65	< 0.01**
Bering Sea	Bliss	Day of Advance	0.4	0.43	< 0.01**
Bering Sea	Bliss	Day of Closing	0.4	0.36	0.02*
Bering Sea	Bliss	Day of Opening	-0.2	-0.28	0.09
Bering Sea	Bliss	Day of Retreat	-0.3	-0.37	0.02*
Bering Sea	J&E	Break-up End	-0.0	-0.01	0.98
Bering Sea	J&E	Break-up Start	0.0	0.05	0.77
Bering Sea	J&E	Freeze-up End	0.3	0.33	0.04*
Bering Sea	J&E	Freeze-up Start	0.5	0.65	< 0.01**
Canadian Arch.	Bliss	Day of Advance	0.5	0.63	< 0.01**
Canadian Arch.	Bliss	Day of Closing	0.6	0.56	< 0.01**
Canadian Arch.	Bliss	Day of Opening	-0.3	-0.57	< 0.01**
Canadian Arch.	Bliss	Day of Retreat	-0.9	-0.7	< 0.01**
Canadian Arch.	J&E	Break-up End	-0.4	-0.62	< 0.01**
Canadian Arch.	J&E	Break-up Start	-0.4	-0.5	< 0.01**
Canadian Arch.	J&E	Freeze-up End	0.3	0.58	< 0.01**
Canadian Arch.	J&E	Freeze-up Start	0.2	0.51	< 0.01**
Central Arctic	Bliss	Day of Closing	0.7	0.33	0.04*
Central Arctic	Bliss	Day of Opening	-0.5	-0.17	0.31
Central Arctic	J&E	Break-up End	-1.0	-0.36	0.03*
Central Arctic	J&E	Break-up Start	-0.9	-0.31	0.06
Central Arctic	J&E	Freeze-up End	0.1	0.03	0.88
Central Arctic	J&E	Freeze-up Start	0.6	0.18	0.31
Chukchi Sea	Bliss	Day of Advance	1.0	0.75	< 0.01**
Chukchi Sea	Bliss	Day of Closing	1.1	0.73	< 0.01**

Chukchi Sea	Bliss	Day of Opening	-0.7	-0.71	< 0.01**
Chukchi Sea	Bliss	Day of Retreat	-0.7	-0.66	< 0.01**
Chukchi Sea	J&E	Break-up End	-0.6	-0.65	< 0.01**
Chukchi Sea	J&E	Break-up Start	-0.5	-0.46	< 0.01**
Chukchi Sea	J&E	Freeze-up End	0.8	0.69	< 0.01**
Chukchi Sea	J&E	Freeze-up Start	1.0	0.79	< 0.01**
E. Siberian Sea	Bliss	Day of Advance	0.8	0.74	< 0.01**
E. Siberian Sea	Bliss	Day of Closing	1.1	0.78	< 0.01**
E. Siberian Sea	Bliss	Day of Opening	-0.7	-0.51	< 0.01**
E. Siberian Sea	Bliss	Day of Retreat	-0.8	-0.6	< 0.01**
E. Siberian Sea	J&E	Break-up End	-0.5	-0.45	< 0.01**
E. Siberian Sea	J&E	Break-up Start	-0.7	-0.46	< 0.01**
E. Siberian Sea	J&E	Freeze-up End	0.6	0.76	< 0.01**
E. Siberian Sea	J&E	Freeze-up Start	0.7	0.77	< 0.01**
Greenland Sea	Bliss	Day of Advance	0.9	0.62	< 0.01**
Greenland Sea	Bliss	Day of Closing	0.5	0.45	< 0.01**
Greenland Sea	Bliss	Day of Opening	-0.4	-0.38	0.02*
Greenland Sea	Bliss	Day of Retreat	-0.6	-0.5	< 0.01**
Greenland Sea	J&E	Break-up End	-0.3	-0.32	0.05*
Greenland Sea	J&E	Break-up Start	-0.0	-0.04	0.79
Greenland Sea	J&E	Freeze-up End	0.4	0.38	0.02*
Greenland Sea	J&E	Freeze-up Start	0.7	0.63	< 0.01**

Hudson Bay	Bliss	Day of Advance	0.5	0.64	< 0.01**
Hudson Bay	Bliss	Day of Closing	0.4	0.57	< 0.01**
Hudson Bay	Bliss	Day of Opening	-0.5	-0.67	< 0.01**
Hudson Bay	Bliss	Day of Retreat	-0.7	-0.74	< 0.01**
Hudson Bay	J&E	Break-up End	-0.4	-0.65	< 0.01**
Hudson Bay	J&E	Break-up Start	-0.1	-0.06	0.72
Hudson Bay	J&E	Freeze-up End	0.4	0.55	< 0.01**
Hudson Bay	J&E	Freeze-up Start	0.6	0.73	< 0.01**
Kara Sea	Bliss	Day of Advance	0.7	0.63	< 0.01**
Kara Sea	Bliss	Day of Closing	0.9	0.66	< 0.01**
Kara Sea	Bliss	Day of Opening	-1.0	-0.75	< 0.01**
Kara Sea	Bliss	Day of Retreat	-1.1	-0.76	< 0.01**
Kara Sea	J&E	Break-up End	-0.9	-0.7	< 0.01**
Kara Sea	J&E	Break-up Start	-0.3	-0.22	0.18
Kara Sea	J&E	Freeze-up End	0.8	0.62	< 0.01**
Kara Sea	J&E	Freeze-up Start	0.7	0.64	< 0.01**
Laptev Sea	Bliss	Day of Advance	0.6	0.65	< 0.01**
Laptev Sea	Bliss	Day of Closing	0.7	0.64	< 0.01**
Laptev Sea	Bliss	Day of Opening	-0.6	-0.55	< 0.01**
Laptev Sea	Bliss	Day of Retreat	-0.7	-0.58	< 0.01**
Laptev Sea	J&E	Break-up End	-0.6	-0.52	< 0.01**
Laptev Sea	J&E	Break-up Start	-0.7	-0.48	< 0.01**
Laptev Sea	J&E	Freeze-up End	0.4	0.68	< 0.01**
Laptev Sea	J&E	Freeze-up Start	0.4	0.64	< 0.01**

Table S3. Same as Table S2, but for the local indicators. Slopes (linear regression lines) correspond to Figures 8-11. Also shown are the explained variances (r^2 values of the trend lines and their levels of statistical significance.

Location	Indicator Group	Indicator	Slope (days yr ⁻¹)	r ²	Significance level
Churchill	Bliss	Day of Advance	0.3	0.52	< 0.01**
Churchill	Bliss	Day of Closing	0.4	0.51	< 0.01**
Churchill	Bliss	Day of Opening	-0.8	-0.59	< 0.01**
Churchill	Bliss	Day of Retreat	-1.0	-0.67	< 0.01**
Churchill	J&E	Break-up End	-0.7	-0.54	< 0.01**
Churchill	J&E	Break-up Start	-0.5	-0.3	0.07
Churchill	J&E	Freeze-up End	0.4	0.49	< 0.01**
Churchill	J&E	Freeze-up Start	0.7	0.53	< 0.01**
Clyde River	Bliss	Day of Advance	0.3	0.46	< 0.01**
Clyde River	Bliss	Day of Closing	0.3	0.45	< 0.01**
Clyde River	Bliss	Day of Opening	-0.6	-0.47	< 0.01**
Clyde River	Bliss	Day of Retreat	-0.5	-0.42	< 0.01**
Clyde River	J&E	Break-up End	-0.6	-0.5	< 0.01**
Clyde River	J&E	Break-up Start	-0.5	-0.22	0.18
Clyde River	J&E	Freeze-up End	0.3	0.45	< 0.01**
Clyde River	J&E	Freeze-up Start	0.3	0.43	< 0.01**
Mestersvig	Bliss	Day of Advance	0.6	0.36	0.05*
Mestersvig	Bliss	Day of Closing	0.9	0.52	< 0.01**
Mestersvig	Bliss	Day of Opening	-0.7	-0.36	0.02*
Mestersvig	Bliss	Day of Retreat	-0.6	-0.37	0.04*
Mestersvig	J&E	Break-up End	-0.2	-0.2	0.26
Mestersvig	J&E	Break-up Start	0.1	0.04	0.83

Formatted: Font: (Default) Times New Roman, 12 pt

Formatted Table

Mestersvig	J&E	Freeze-up End	0.6	0.5	< 0.01**
Mestersvig	J&E	Freeze-up Start	0.5	0.42	0.02*
Pevek	Bliss	Day of Advance	1.1	0.72	< 0.01**
Pevek	Bliss	Day of Closing	1.1	0.77	< 0.01**
Pevek	Bliss	Day of Opening	-0.9	-0.4	0.01*
Pevek	Bliss	Day of Retreat	-1.0	-0.46	< 0.01**
Pevek	J&E	Break-up End	-0.7	-0.33	0.05
Pevek	J&E	Break-up Start	-1.1	-0.37	0.03*
Pevek	J&E	Freeze-up End	0.8	0.76	< 0.01**
Pevek	J&E	Freeze-up Start	0.9	0.73	< 0.01**
Prudhoe Bay	Bliss	Day of Advance	0.8	0.52	< 0.01**
Prudhoe Bay	Bliss	Day of Closing	0.8	0.65	< 0.01**
Prudhoe Bay	Bliss	Day of Opening	-1.0	-0.56	< 0.01**
Prudhoe Bay	Bliss	Day of Retreat	-0.9	-0.51	< 0.01**
Prudhoe Bay	J&E	Break-up End	-0.8	-0.54	< 0.01**
Prudhoe Bay	J&E	Break-up Start	-0.5	-0.27	0.1
Prudhoe Bay	J&E	Freeze-up End	0.8	0.6	< 0.01**
Prudhoe Bay	J&E	Freeze-up Start	0.7	0.59	< 0.01**
Sabetta	Bliss	Day of Advance	0.4	0.55	< 0.01**
Sabetta	Bliss	Day of Closing	0.4	0.47	< 0.01**
Sabetta	Bliss	Day of Opening	-0.9	-0.59	< 0.01**
Sabetta	Bliss	Day of Retreat	-1.0	-0.78	< 0.01**
Sabetta	J&E	Break-up End	-0.8	-0.56	< 0.01**
Sabetta	J&E	Break-up Start	-0.9	-0.42	< 0.01**
Sabetta	J&E	Freeze-up End	0.4	0.41	< 0.01**
Sabetta	J&E	Freeze-up Start	0.4	0.56	< 0.01**

South Chukchi Sea	Bliss	Day of Advance	0.9	0.63	< 0.01**
South Chukchi Sea	Bliss	Day of Closing	0.7	0.58	< 0.01**
South Chukchi Sea	Bliss	Day of Opening	-0.6	-0.51	< 0.01**
South Chukchi Sea	Bliss	Day of Retreat	-0.7	-0.56	< 0.01**
South Chukchi Sea	J&E	Break-up End	-0.6	-0.52	< 0.01**
South Chukchi Sea	J&E	Break-up Start	-0.6	-0.39	0.02*
South Chukchi Sea	J&E	Freeze-up End	0.7	0.57	< 0.01**
South Chukchi Sea	J&E	Freeze-up Start	0.8	0.63	< 0.01**
St. Lawrence Island	Bliss	Day of Advance	0.6	0.33	0.05*
St. Lawrence Island	Bliss	Day of Closing	0.3	0.2	0.24
St. Lawrence Island	Bliss	Day of Opening	-0.1	-0.16	0.35
St. Lawrence Island	Bliss	Day of Retreat	-0.3	-0.28	0.09
St. Lawrence Island	J&E	Break-up End	-0.1	-0.11	0.49
St. Lawrence Island	J&E	Break-up Start	-0.0	-0.02	0.92
St. Lawrence Island	J&E	Freeze-up End	0.4	0.25	0.13
St. Lawrence Island	J&E	Freeze-up Start	0.5	0.33	0.04*
Tiksi	Bliss	Day of Advance	0.2	0.36	0.02*
Tiksi	Bliss	Day of Closing	0.2	0.41	0.01*

Tiksi	Bliss	Day of Opening	-0.4	-0.54	< 0.01**
Tiksi	Bliss	Day of Retreat	-0.6	-0.54	< 0.01**
Tiksi	J&E	Break-up End	-0.3	-0.53	< 0.01**
Tiksi	J&E	Break-up Start	-0.3	-0.34	0.03*
Tiksi	J&E	Freeze-up End	0.3	0.45	< 0.01**
Tiksi	J&E	Freeze-up Start	0.2	0.45	< 0.01**
Utqiaf°vik	Bliss	Day of Advance	1.1	0.6	< 0.01**
Utqiaf°vik	Bliss	Day of Closing	1.1	0.67	< 0.01**
Utqiaf°vik	Bliss	Day of Opening	-1.2	-0.52	< 0.01**
Utqiaf°vik	Bliss	Day of Retreat	-1.2	-0.71	< 0.01**
Utqiaf°vik	J&E	Break-up End	-0.7	-0.52	< 0.01**
Utqiaf°vik	J&E	Break-up Start	-0.7	-0.27	0.11
Utqiaf°vik	J&E	Freeze-up End	0.8	0.66	< 0.01**
Utqiaf°vik	J&E	Freeze-up Start	0.9	0.62	< 0.01**

Formatted: Font: (Default) Times New Roman, 12 pt